Cross-linked, Porous Imidazolium-based Poly(Ionic Liquid)s for CO_2 Capture and Utilisation

Ala'a F. Eftaiha,[a] Abdussalam K. Qaroush,*[b] Areej K. Hasan,[b] Khaleel I. Assaf,[c] Feda'a M. Al-Qaisi,[a] Maryam E. Melhem,[b] Bassem A. Al-Maythalony,[d,e] Muhammad Usman[f]*

[a] Department of Chemistry, Faculty of Science, The Hashemite University, P.O. Box 330127, Zarqa 13133, Jordan. E-mail: alaa.eftaiha@hu.edu.jo
[b] Department of Chemistry, Faculty of Science, The University of Jordan, Amman 11942, Jordan. E-mail: a.qaroush@ju.edu.jo
[c] Department of Chemistry, Faculty of Science, Al-Balqa Applied University, Al-Salt 19117, Jordan.
[d] Materials Discovery Research Unit, Advanced Research Centre, Royal Scientific Society, Amman 11941, Jordan.
[e] Technology Innovation Center on Carbon Capture and Sequestration (TIC-CCS), King Fahd University of Petroleum and Minerals (KFUPM), Dhahran, 31261, Saudi Arabia.
[f] Center of Research Excellence in Nanotechnology (CENT), King Fahd University of Petroleum and Minerals (KFUPM), Dhahran 31261, Saudi Arabia.

Electronic Supplementary Information (ESI)

Table S1. CO_2 sorption performance of imidazolium based PILs.

PILs	Acronym	Sorption Conditions *T* (K)/ *P* (bar)	CO_2 Uptake[a]	Ref
3-(4-vinylbenzyl)-1-vinylimidazolium bis(trifluoro methylsulfonyl)- imide	VBIm-IL	273 /1	0.02	1
m-poly-3-(4-vinylbenzyl)-1-vinylimidazolium bis(trifluoro methylsulfonyl)- imide	*m*-PIL	273 /1	0.46	1
m-poly(3-N-hexyl-1-vinylimidazolium bromide	*co*-PVI-C6	295 /1	0.18	2
Poly(N-vinylimidazole bromide)	PVEIm[Br]	295 /1	0.09	3
Poly(N-vinylimidazole tetrafluroborate)	PVEIm[BF_4]	295 /1	0.12	3
Poly(N-vinylimidazole hexafluorophosphate)	PVEIm[PF_6]	295 /1	0.13	3
Urea-functionalised imidazolium-based ionic polymer	UIIP	273	0.418	4
Click-based porous organic polymer bearing imidazolium IL	CPP-ILs	273/1	2.13	5
Poly(1,2,3,4,5,6-hexakis (methyl) benzene vinylimidazolium bromide)	PVImBr-6-SCD	273 /1	3.60	6
2-Phenylimidazolinium based porous hyper crosslinked ionic Polymers	HIP-Br-2	273/1	2.9	7
	HIP-Cl-1		3.8	

[a] The unit of CO_2 uptake is "mmol CO_2/g sorbent"

1. Synthesis of Monomers

1.1.Synthesis of 3-(3-(phthalimide)propyl)-1-vinylimidazolium bromide (**3**)

1-vinylimidazole, (**1**, 1.04 g, 0.011 mol) was added to a solution of N-(3-bromopropyl)phthalimide, (**2**, 3.50 g, 0.011 mol) in 10 mL toluene and heated up to (70-75) °C with continuous stirring for 24 h (**Scheme 1**). The white precipitate (**3**) was filtered and washed with 4 × 20 mL DCM portions, and then dried in a vacuum for 4 h. The obtained yield was 85%. ^{1}H NMR (400 MHz, DMSO) δ 9.58 (s, 1H), 8.25 (s, 1H), 7.96 (s, 1H), 7.86 (s, 4H), 7.33 (dd, 1H), 5.98 (d, *J* = 15.6 Hz, 1H), 5.42 (d, *J* = 8.0 Hz, 1H), 4.28 (t, 2H), 3.63 (t, 2H), 2.21 (q, 2H). ^{13}C NMR (101 MHz, DMSO) δ 168.03, 135.55, 134.42, 131.67, 128.85, 123.17, 123.03, 119.15, 108.70, 46.94, 39.52, 34.30, 28.35. EA, Calculated: C: 53.05; H:

4.45 and N: 11.60. Found: C: 53.90; H: 5.31 and N: 11.59. ATR-FTIR (500-4000) cm^{-1} range, 1765 ($C=O_{asym}$), 1710 ($C=O_{sym}$), 1649 ($C=C_{vinyl}$), 1618 ($C=C_{Ar}$), 1572, 1553 ($C=N^{+}$), 532 (C-Br). m.p.: 190 °C.

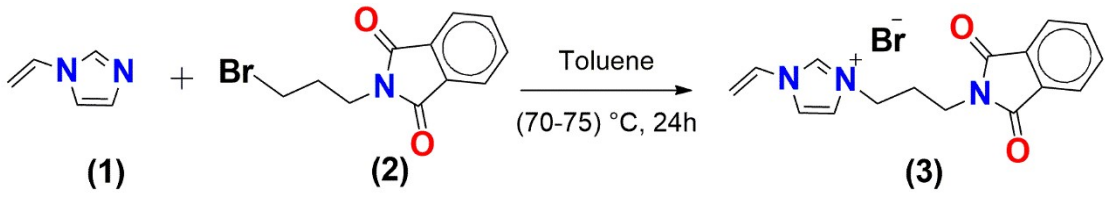

Scheme S1. The synthetic route of imidazolium-based monomer (**3**)

1.2.Synthesis of N-allylphthalimide (**6**)

The N-allylphthalimide was synthesised as previously reported [8]. Allyl chloride (**4**, 2.0 mL, 0.025 mol) was added to a mixture of potassium phthalimide (**5**, 5.0 g, 0.027 mol) and TBAB (1.0 g, 0.003 mol) in 17 mL DMF (**Scheme 2**). The reaction mixture was heated up to 55 °C for 24h. Later, a yellow oily layer was washed with deionized water to get rid of any unreacted starting materials. The white solid product **6** was dried in a vacuum oven for 4 h. The separated yield was 76%. ^{1}H NMR (500 MHz, DMSO) δ 7.84 (m, 4H), 5.88 (m, 1H), 5.13 (s, 1H), 5.10 (d, J = 5.8 Hz, 1H), 4.17 (d, 2H). ^{13}C NMR (126 MHz, DMSO) δ 167.45, 134.43, 132.39, 131.54, 123.07, 116.31. EA Calculated: C: 70.58; H: 4.85 and N: 7.48. Found, C: 70.64; H: 5.61 and N: 7.43. ATR-FTIR (500-4000) cm^{-1} range, 1770 ($C{=}O_{asym}$), 1690 ($C{=}O_{sym}$), 1645 ($C{=}C_{allyl}$), 1620 ($C{=}C_{Ar}$). m.p.: 76 °C.

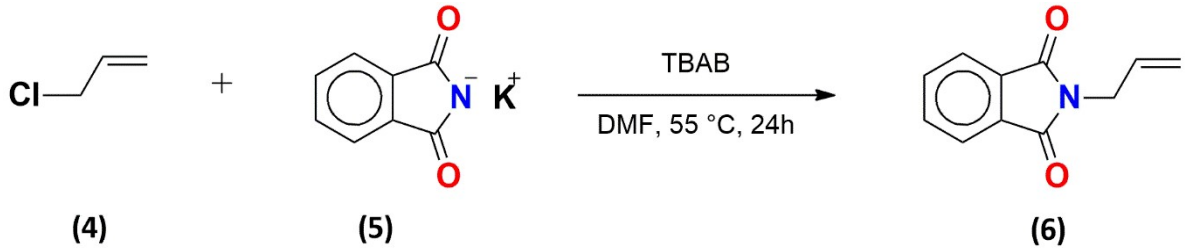

Scheme S2. Synthesis of N-allylphthalimide (**6**)

2. Synthesis of Copolymers

2.1.Synthesis of *co*-poly(3-(3-(phthalimide) propyl)-1-vinylimidazolium bromide)(N-allylphthalimide), (*co*-PIL-x1, **7**)

The *co*-PIL-x1 (**7**) was prepared *via* free radical polymerisation of the synthesised IL precursor and N-allylphthalimide using DVB as a crosslinker and AIBN as an initiator (**Scheme 3**). A mixture of **3** (0.36 g, 0.001 mol) and **6** (0.19 g, 0.001 mol) were added to a solution of DVB (2 mL, 0.014 mol) in 17 mL DMSO. The solution was sonicated at 40°C for 1h. Consequently, a solution of the initiator, (0.2 M of an AIBN in 1 ml of toluene; 0.007

mol) was added to the reaction mixture under N_2, and then the reaction was heated up to 70°C for 24 h. A white fine powder was collected, soaked and washed with DCM and finally dried in the oven. The isolated yield was 50%.

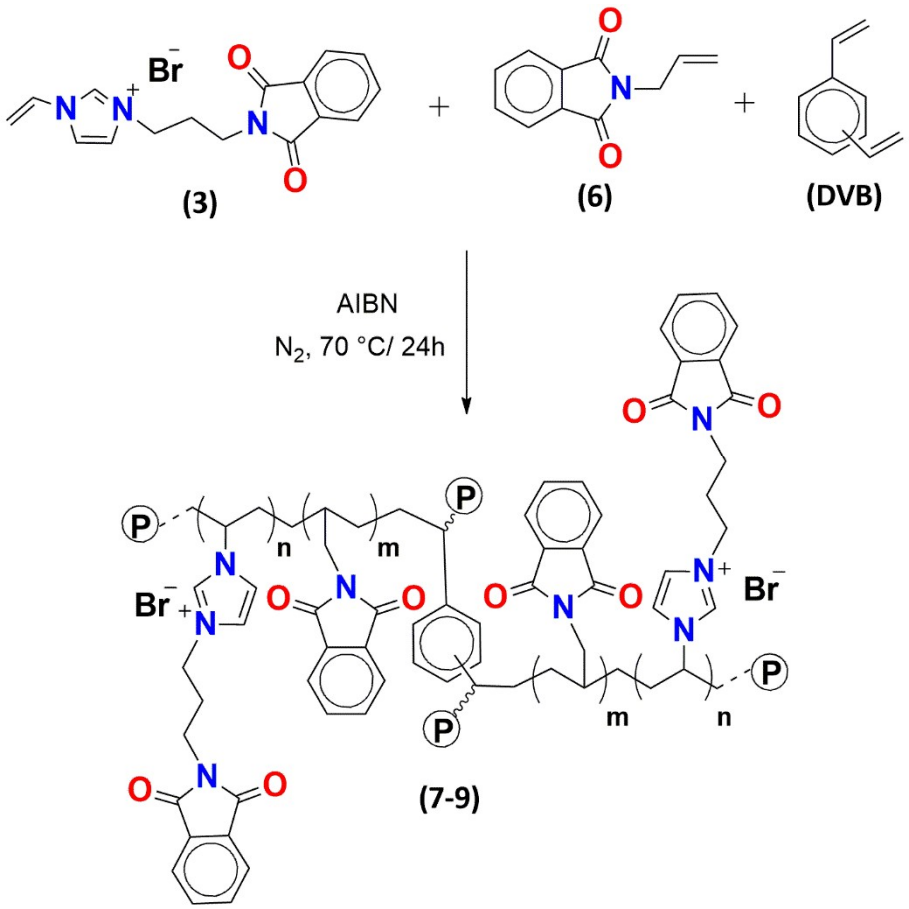

Scheme S3. Synthesis of *co*-PIL-xy (y: 1, 2 or 4, **7-9**) as a result of random polymerisation of **3** and **6** and simultaneous crosslinking using DVB.

2.2.Synthesis of *co*-PIL-x2 (**8**) and *co*-PIL-x4 (**9**)

The synthetic protocols of *co*-PIL-x2 (**8**) and *co*-PIL-x4 (**9**), were done by following the previous co-PIL-x1 (**7**) synthesis procedure; employing different molar ratio of the monomers which was doubled in **8** and quadruple in **9**. Consequently, a (**3**, 0.72 g, 0.002 mol) and (**6**, 0.38 g, 0.002 mol) for **8**, while (**3**, 1.44 g, 0.004 mol) and (**6**, 0.76 g, 0.004 mol) for **9**. The percentage yields were 64 and 89%, respectively.

2.3.Synthesis of *co*-poly(3-(3-(propylamine)-1-vinyl-imidazol-3-ium bromide)(N-allylamine) (*co*-PIL-NH_2-xy, **10-12**; y = 1, 2, 4)

Hydrazinolysis of **7-9** into their corresponding amines (**10-12**) was achieved upon mixing 1 g of the *co*-PILs with hydrazine hydrate (4 mL, 0.625 mol) in 15 mL ethanol. The mixture was refluxed for 24 h at 90 °C. The solid polymers were washed several times with DMSO to get rid of any phthalhydrazide traces, then washed excessively with ethanol and dried in the oven for 4 h. The yields for 10-12 were 62, 86 and 60%, respectively.

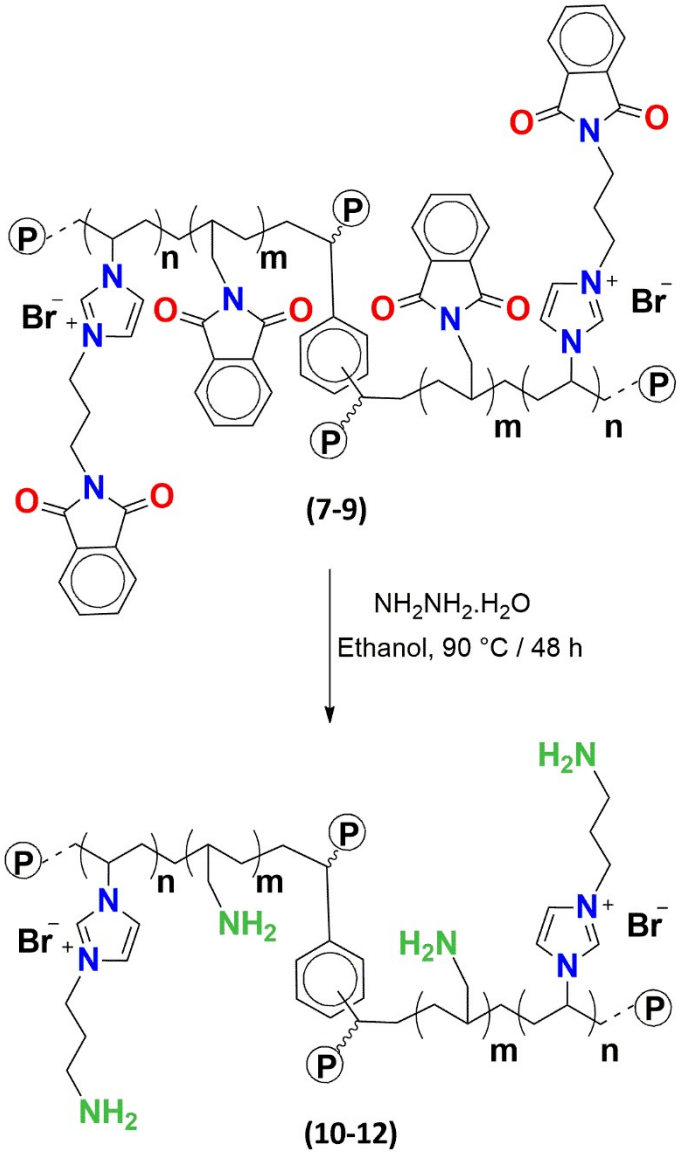

Scheme S4. Hydrazinolysis of the proposed formula of the phthalimide-based PILs (**7-9**) to yield the amine-functionalised *co*-PILs (**10-12**)

3. Synthesis of Homopolymers

3.1. Synthesis of *homo*-poly(3-(3-(phthalimide) propyl)-1-vinylimidazolium bromide), (*homo*-PIL-x1, **13**)

The *homo*-PIL-x1 (**13**) was synthesised by dissolved and sonicated the IL precursor (**3**, 0.36 g, 0.001 mol) in 15 mL of DMSO with DVB (1 mL, 0.007 mol) at 40 °C for 1h. While the solution was kept under N_2, 0.2 M AIBN solution in toluene (1 mL, 0.007 mol) was added to the reaction mixture, and then refluxed up to 70 °C for 24 h (**Scheme S5A**). A very fine powder was collected, soaked and washed with DCM and dried in the oven. The percentage yield was 60%.

3.2. Synthesis of *homo*-PIL-x2 (**14**) and *homo*-PIL-x4 (**15**)

The *homo*-PIL-x2 (**14**) and *homo*-PIL-x4 (**15**) were synthesised by a similar procedure to that of *homo*-PIL-x1 (**13**). Thus, the IL precursor (**3**, 0.72 g, 0.002 mol) was needed to prepare **14**, while the **15** was synthesised from (**3**, 1.44 g, 0.004 mol) as shown in **Scheme 5A**. The fine powders (**14** and **15**) were collected, soaked and washed by DCM and dried in the oven. The yields for **14** and **15** were 74 and 66%, respectively.

3.3. Synthesis of *homo*-poly(N-allylphthalimide), (*homo*-PAP, **17**)

homo-PAP (**17**) was synthesised by dissolving N-allylphthalimide (**6**, 0.19 g, 0.001 mol) in 15.0 mL DMSO mixed with DVB (1.0 mL, 0.007 mol) and sonicated at 40 °C for 1h. Afterwards, 0.2 M AIBN solution in toluene (1 mL, 0.007 mol) was added to the reaction mixture under N_2 and then refluxed for 24 h at 70 °C (**Scheme 5B**). The consequential the fine powder was collected, soaked and washed with DCM and dried in the oven for 4 h. The percentage yield was 57%.

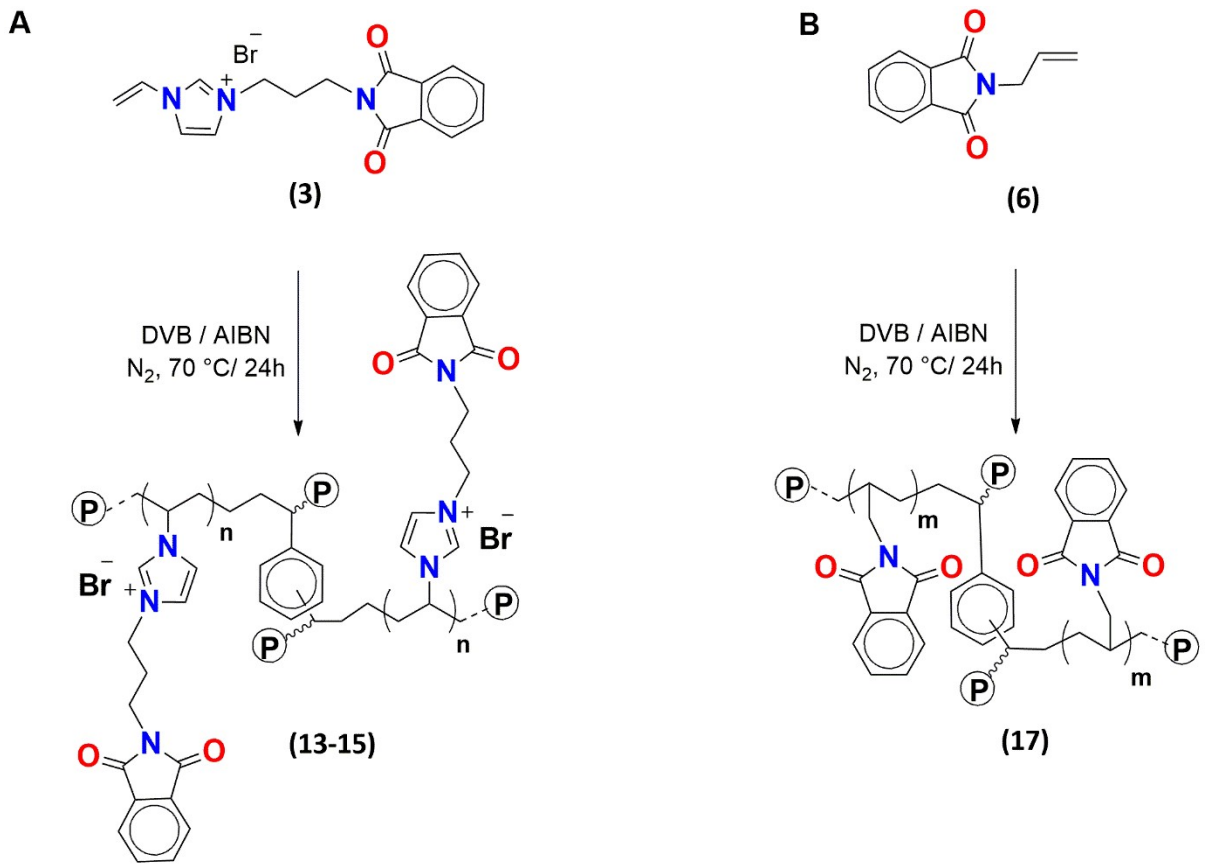

Scheme S5. Synthesis of: **A.** *homo*-PILs (**13-15**) *via* free radical polymerisation of **3**, **B.** *homo*-PAP (**17**) starting with **6**

4. Synthesis of Amine-Terminated *homo*-polymers

4.1. Synthesis of poly(3-(3-(propylamine)-vinylimidazolium bromide); *homo*-PIL-NH_2-x1 (**16**):

The mixture of *homo*-PIL-NH_2-x1 (**13**, 1.0 g) and NH_2NH_2•H_2O (4 mL, 0.019 mol) in 15 mL ethanol was refluxed at 90 °C for 48 h (**Scheme 6A**). The solid was collected, washed several times with abundant amounts of DMSO/ethanol to get rid of any by-products and dried in oven. The yield was 68%.

4.2. Synthesis of *homo*-poly(N-allylamine) (*homo*-PAA, **18**):

A mixture of *homo*-PAP (**17**, 1.0 g) and an excess amount of NH_2NH_2•H_2O (4 mL, 0.019 mol) in 15 mL ethanol was refluxed at 90 °C for 48 h (**Scheme 6B**). Afterwards, the solid

was collected, washed with copious amount of DMSO/ethanol several times and dried in oven. The yield was 74%.

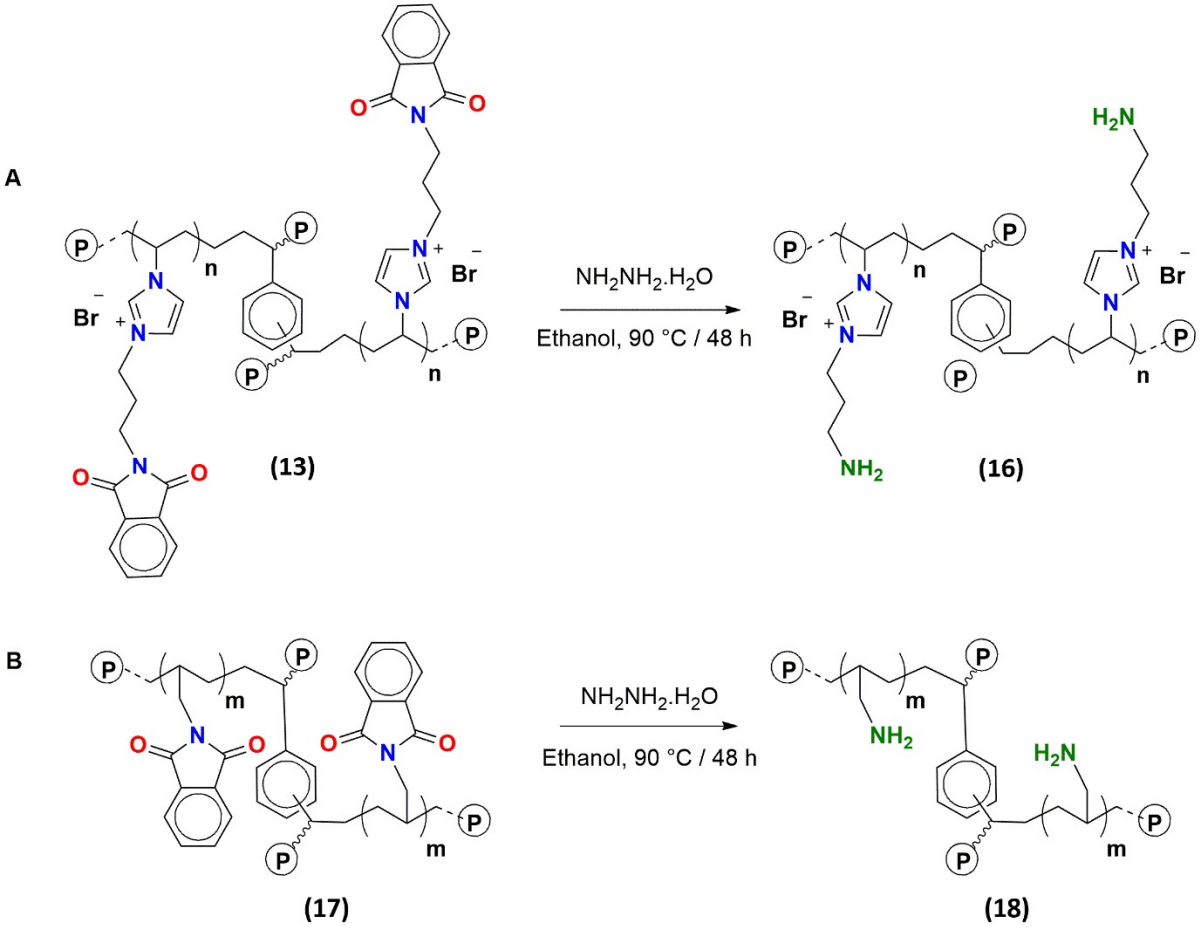

Scheme S6. Synthesis of *homo*-PIL-NH_2-x1 (**16**) and *homo*-PAA (**18**)

Table S2. The synthesised monomeric analogues and *homo*-/co-polymers yields.

Samples	Code	Yields %
1-Vinylimidazole	**1**	-
N-(3-bromopropyl)phthalimide	**2**	-
IL precursor	**3**	85
Allyl chloride	**4**	-
Potassium phthalimide	**5**	-
N-allylphthalimide	**6**	76
co-PIL-x1	**7**	50
co-PIL-x2	**8**	64
co-PIL-x4	**9**	89
co-PIL-NH_2-x1	**10**	62
co-PIL-NH_2-x2	**11**	86
co-PIL-NH_2-x4	**12**	60
homo-PIL-x1	**13**	60
homo-PIL-x2	**14**	74
homo-PIL-x4	**15**	66
homo-PIL-NH_2-x1	**16**	68
homo-PAP	**17**	57
homo-PAA	**18**	74

5. Materials' Characterisation

5.1. Characterisation of 3-(3-(phthalimide)propyl)-1-vinylimidazol-3-ium bromide (**3**)

The ^{1}H NMR spectrum of **3** is shown in **Figure S1**. The most down-fielded singlet peak at 9.58 ppm (**a**) corresponding to the hydrogen on the imidazolium head which verified the quaternarisation process.[9] The two singlet peaks observed at 8.25 and 7.96 ppm were ascribed to the hydrogens **b** and **c**, respectively.[6] While, the aromatic hydrogens of the phenyl ring in the phthalimide bulk were observed as a singlet peak at 7.86 ppm (**d**). Furthermore, a doublet of doublet peak at 7.34 ppm corresponding to the vinylic hydrogen (**e**) was attained.[10] Two more doublet peaks were observed at 5.98 and 5.42 ppm and assigned to the terminal vinylic hydrogens (**f**).[9] The methylene hydrogens (**g**, **h** and **i**) can be distinguished as two triplets at 4.28, 3.63, and a quintet at 2.21 ppm, respectively.

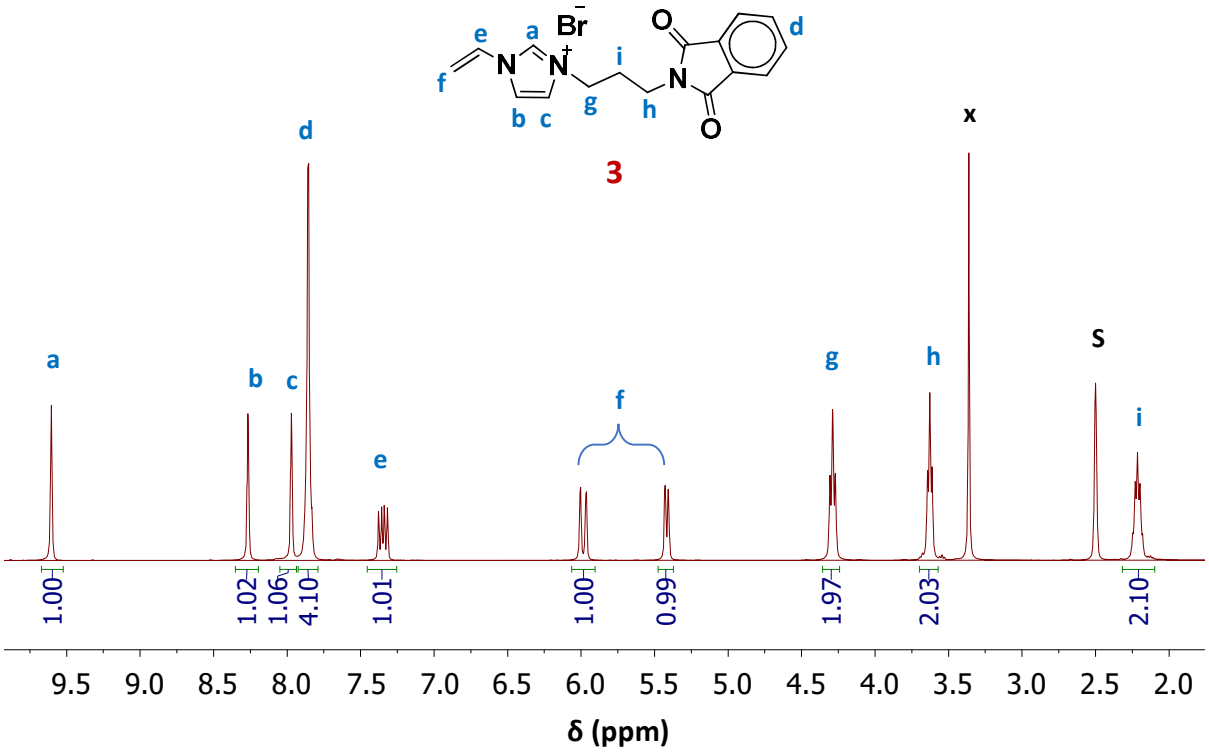

Figure S1. ^{1}H NMR spectrum of **3** in DMSO-d_6; **S**: Solvent; **x**: H_2O.

The ^{13}C NMR of **3** (**Figure S2**) further confirmed the presumed structure. The peaks at 135.6 ppm (**b**), 119.2 and 123.2 ppm (**h** and **f**) revealed the presence of an imidazolium group.[6] Another proof for the inclusion of the vinylic group within **3** was resembled in the emergence of two peaks at 128.9 and 108.7 ppm (**e** and **i**, respectively).[6] The peak at 168.0 ppm (**a**) was assigned to the carbonyl carbon of the phthalimide unit, and the peaks centered at 134.4, 131.7 and 123.0 ppm (**c**, **d** and **g**, respectively) corresponding to the carbon atoms in the benzene ring.[11] Moreover, the peaks at 46.9, 34.3 and 28.4 ppm (**j**, **k** and **l**) indicated the presence of a methylene carbons of the aliphatic chain.

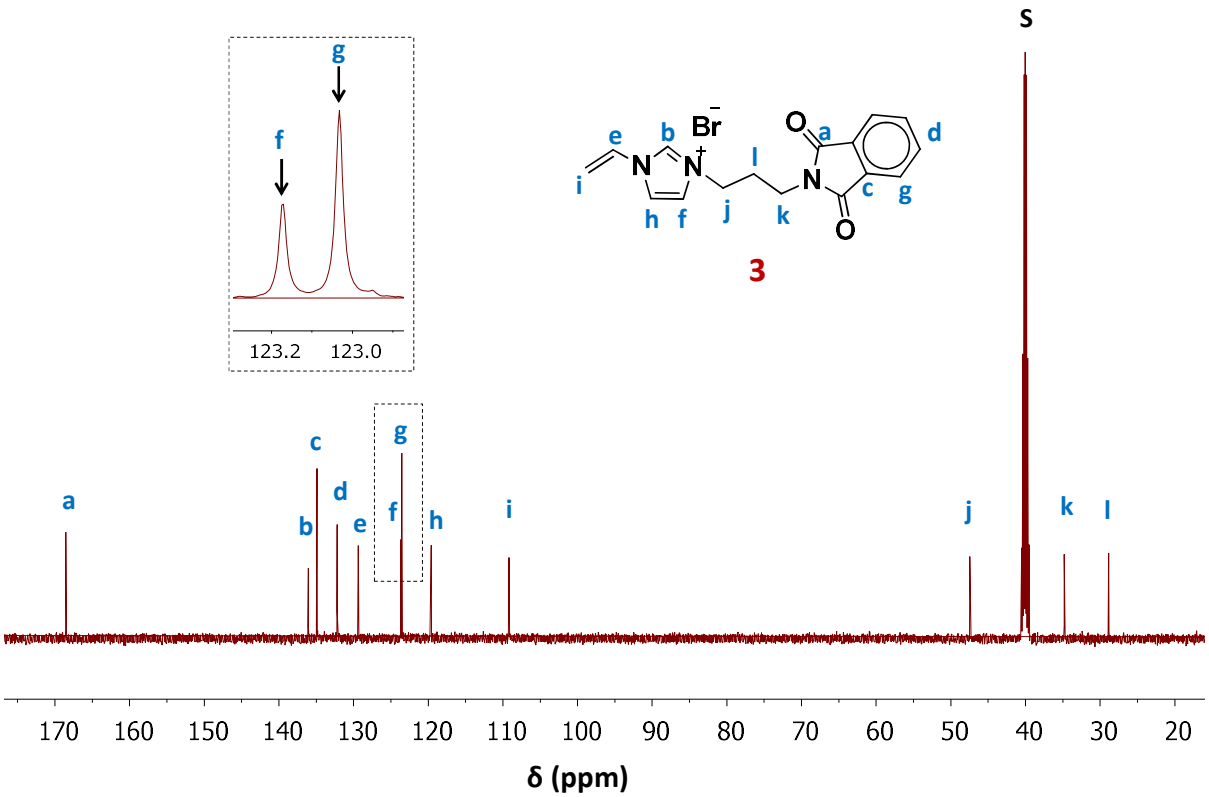

Figure S2. ^{13}C NMR spectrum of **3** in DMSO-d_6; **S**: Solvent.

The ATR-FTIR was used to investigate the main functional groups of the starting materials and the presumed synthesised products. **Figure S3** shows the spectra of 1-vinylimidazole (**1**), N-(3-bromopropyl)phthalimide (**2**), and **3**. The disappearance of C-Br stretching vibration peak in spectrum of **3** at 532 cm^{-1} indicated that the IL was successfully synthesised, in which the peak was observed in the spectrum of **2**.[12] Also, the C=N peaks in the imidazolium ring observed at 1512 and 1487 cm^{-1} were shifted to 1572 and 1553 cm^{-1} in the ATR-FTIR spectrum of **3** due to formation of the positively charged C=N^{+}.[3] The peak assigned to the C=C vinylic group was observed at 1649 cm^{-1}.[3,13] The sharp absorption peak at 725 cm^{-1} was attributed to the rocking mode of =C-H bond.[14] Additionally, two clear absorptions for the asymmetric and symmetric stretching vibrational modes of O=C-N-C=O bonds within the imide functional group were observed at 1767 cm^{-1} and 1710 cm^{-1}, respectively, [15–17] and the

peak of the C=C bond of the benzene ring was observed at 1618 cm^{-1}; these values indicated the presence of the phthalimide groups.[17]

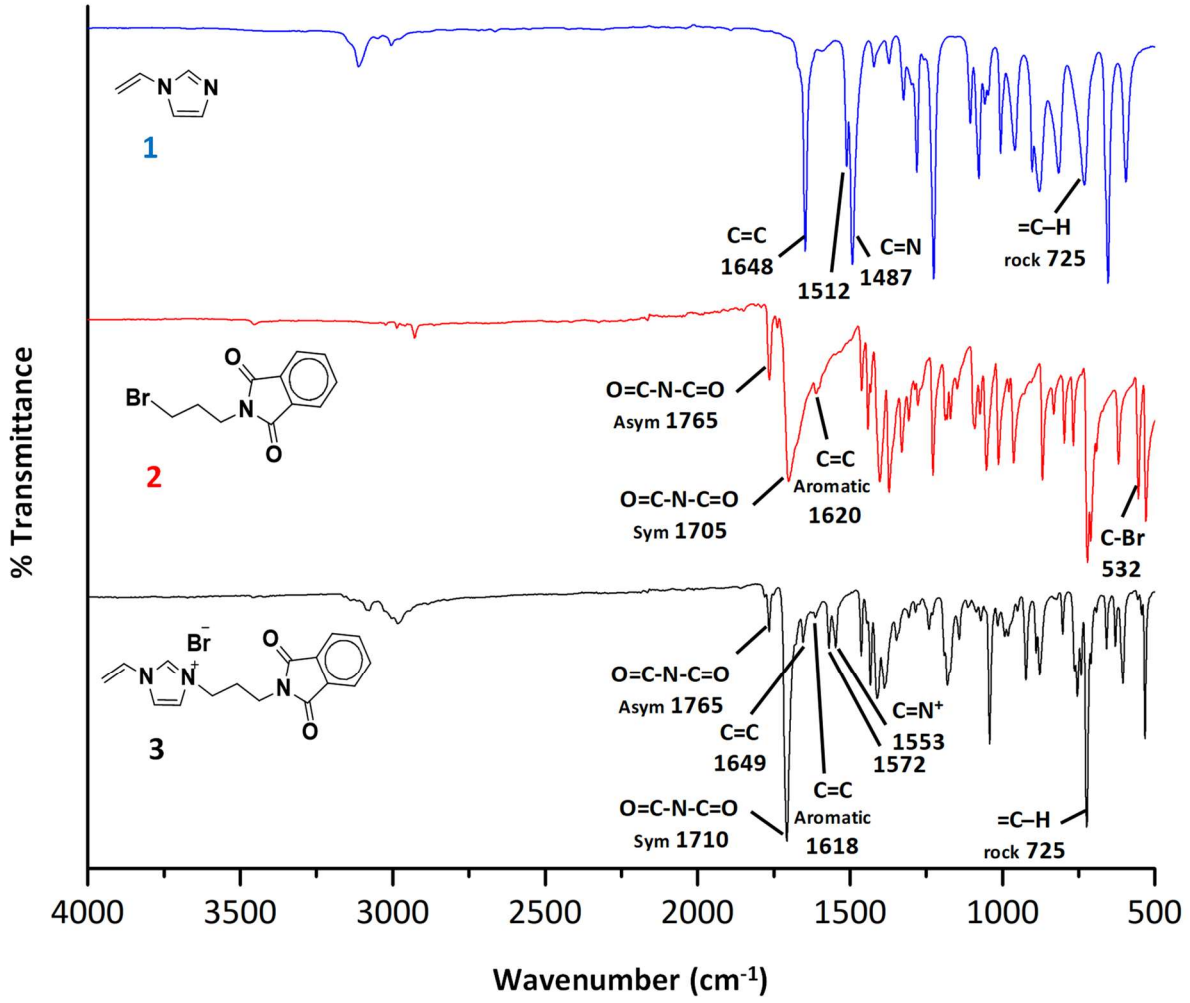

Figure S3. ATR-FTIR spectra of 1-vinylimidazole (**1**, blue trace), N-(3-bromopropyl)phthalimide (**2**, red trace) and the IL precursor (**3**, black trace).

5.2. Characterisation of N-allylphthalimide monomer (**6**)

The aromatic hydrogens of the phthalimide moiety were observed as a multiplet peak at 7.84 ppm (**d**) in the ^{1}H NMR of **6** as shown in **Figure S4**. The vinylic hydrogens appeared as multiplets centered at 5.88 and 5.13 ppm (**c** and **b**). Furthermore, the methylene protons were observed as a distinct doublet at 4.17 ppm (**a**).[18]

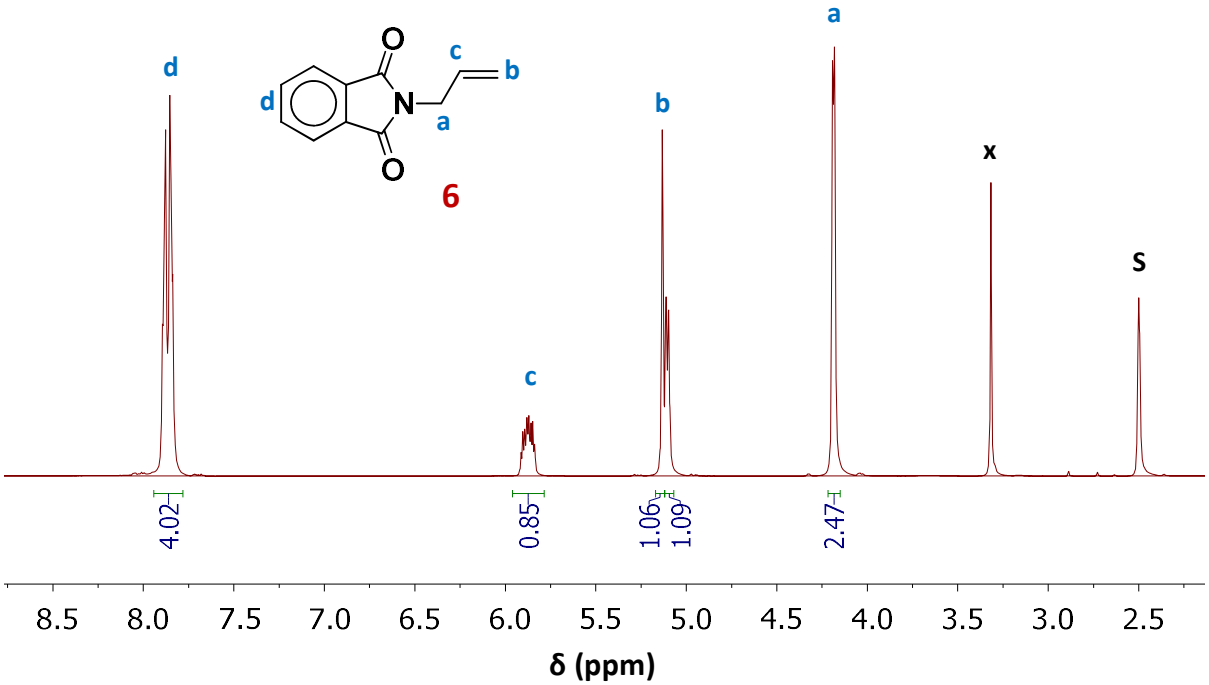

Figure S4. ^{1}H NMR spectrum of **6** in DMSO-d_6; **S**: Solvent; **x**: H_2O.

The ^{13}C NMR spectrum of **6** is shown in **Figure S5**. The observed peak at 167.5 ppm (**a**) was assigned to the carbonyl group of the phthalimide group. The signals for the benzene ring carbons of the corresponding group were observed at 132.4, 131.5 and 123.1 ppm (**c**, **e**, and **d**), respectively. Moreover, the peaks at 134.4 and 116.3 ppm (**b** and **f**) referred to the carbons in the vinylic bond. While, the lowest chemical shift at 39.5 ppm (**g**) referred to the methylene carbon which further verified the structure of **6**.[18]

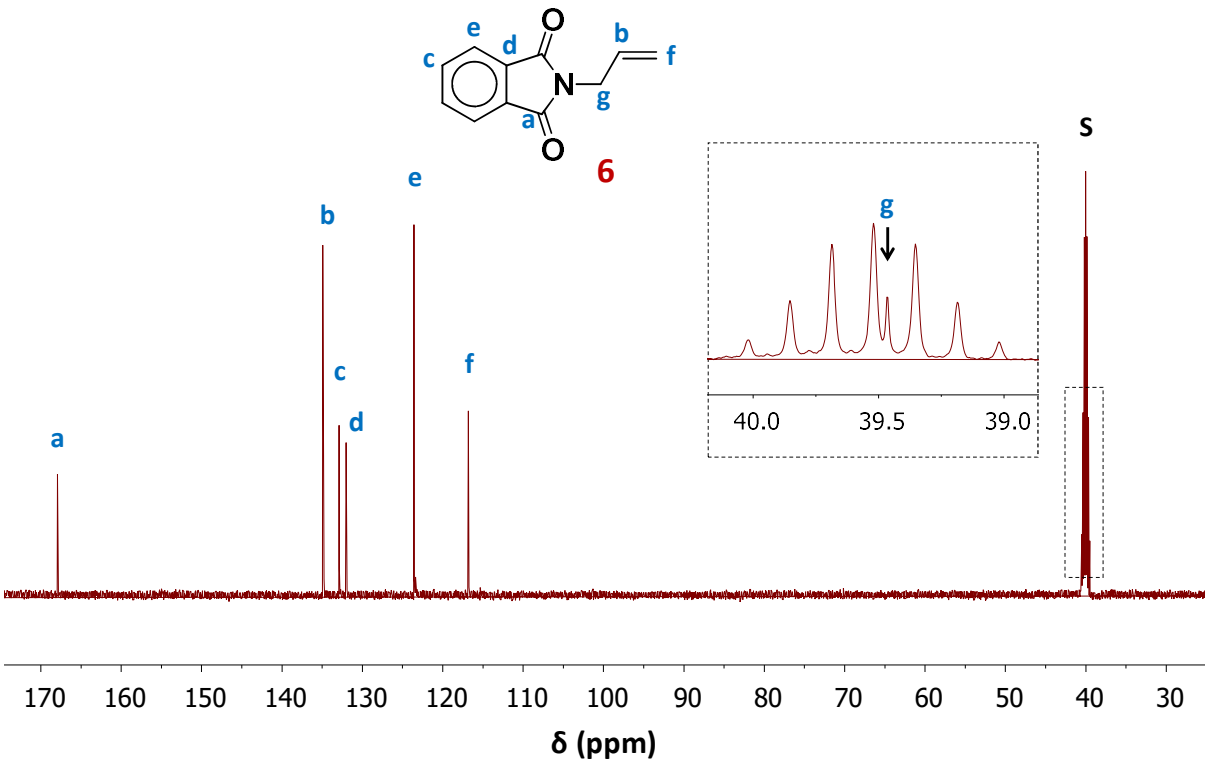

Figure S5. ^{13}C NMR spectrum of **6** in DMSO-d_6; **S**: Solvent.

Figure S6 shows the ATR-FTIR spectra in the 500 to 4000 cm^{-1} range for the allyl chloride (**4**), potassium phthalimide (**5**) and **6**. The disappearance of the C-Cl peak which was observed at 733 cm^{-1} in **4**, indicated a successful quaternarisation process.[19] The characteristic peaks at 1765 and 1697 cm^{-1} were associated with absorptions for the asymmetric and symmetric O=C-N-C=O modes of vibration, respectively.[15] In addition, the benzene ring C=C stretching frequency was observed at 1620 cm^{-1}, indicating the presence of the phthalimide group.[17]

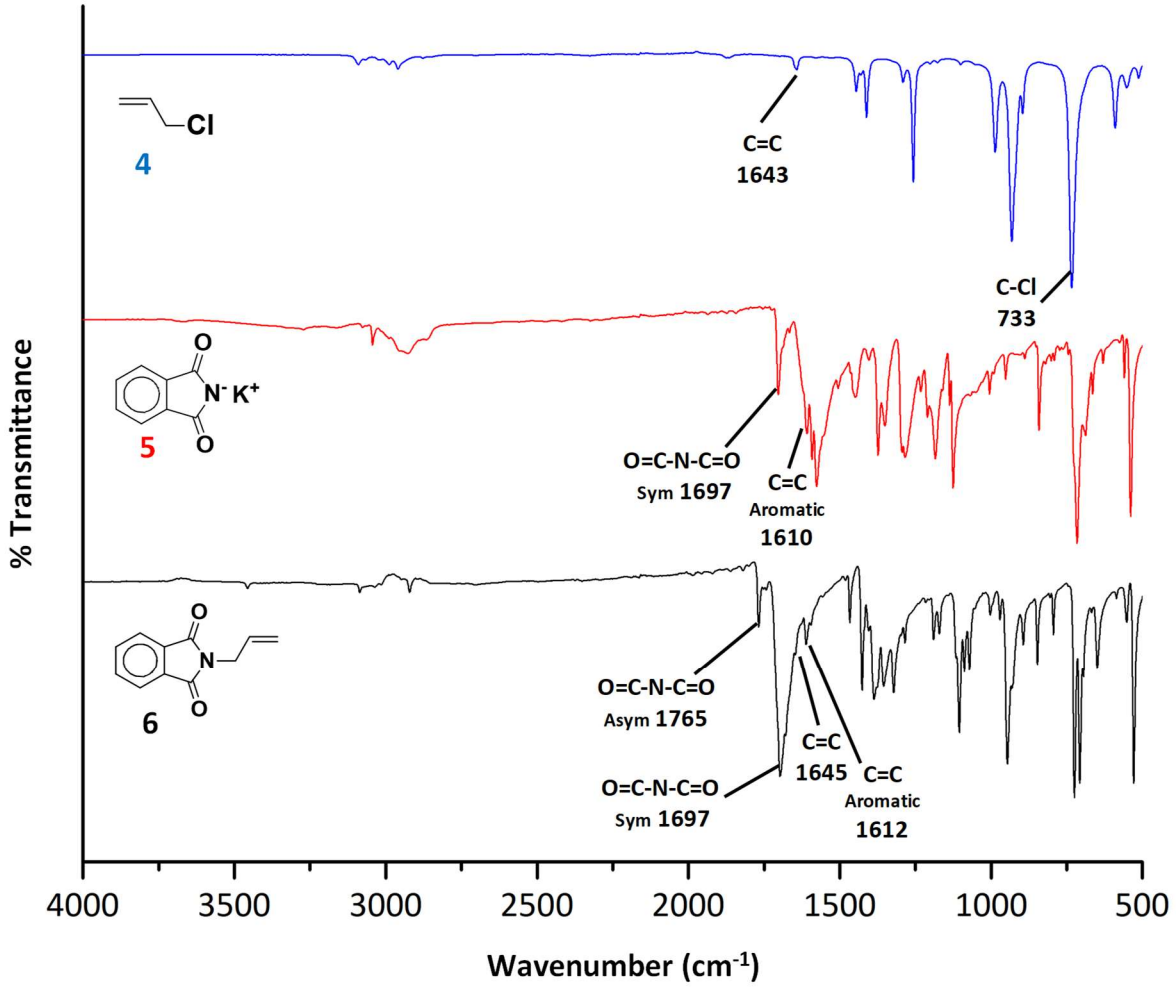

Figure S6. ATR-FTIR spectra of allyl chloride (**4**, blue trace), potassium phthalimide (**5**, red trace) and **6** (black trace).

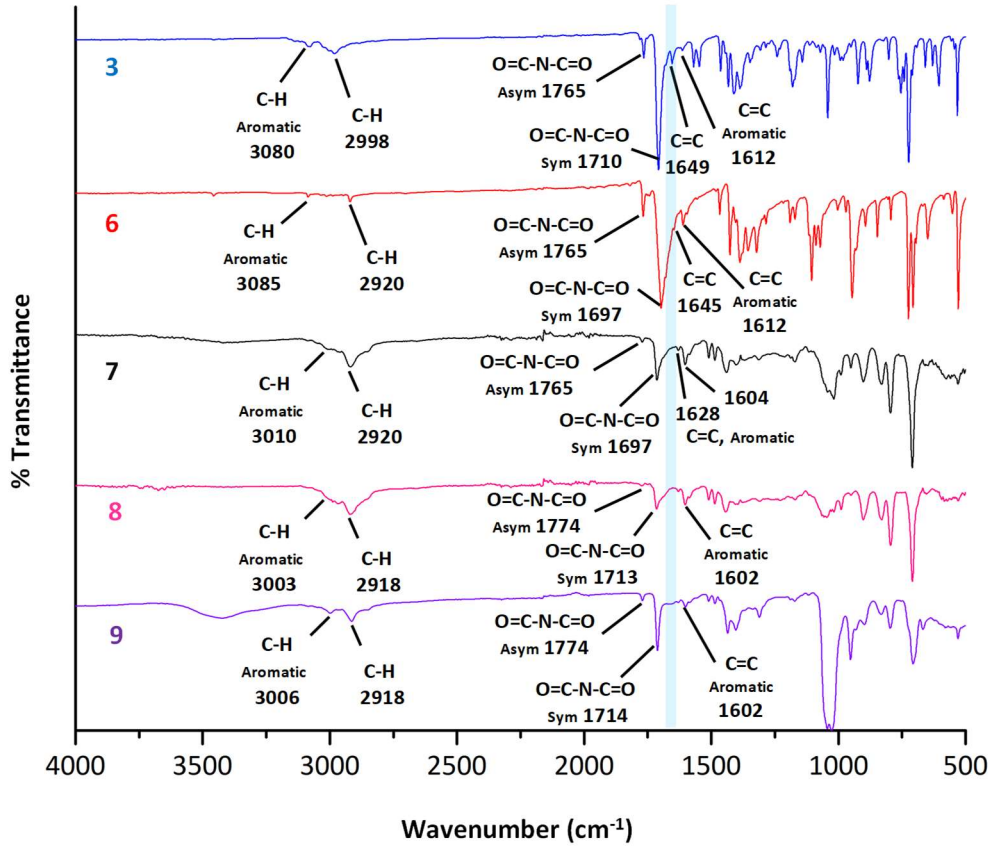

Figure S7. ATR-FTIR spectra of **3** (blue trace), **6** (red trace), *co*-PIL-x1 (**7**, black trace), *co*-PIL-x2 (**8**, pink trace) and *co*-PIL-x4 (**9**, violet trace).

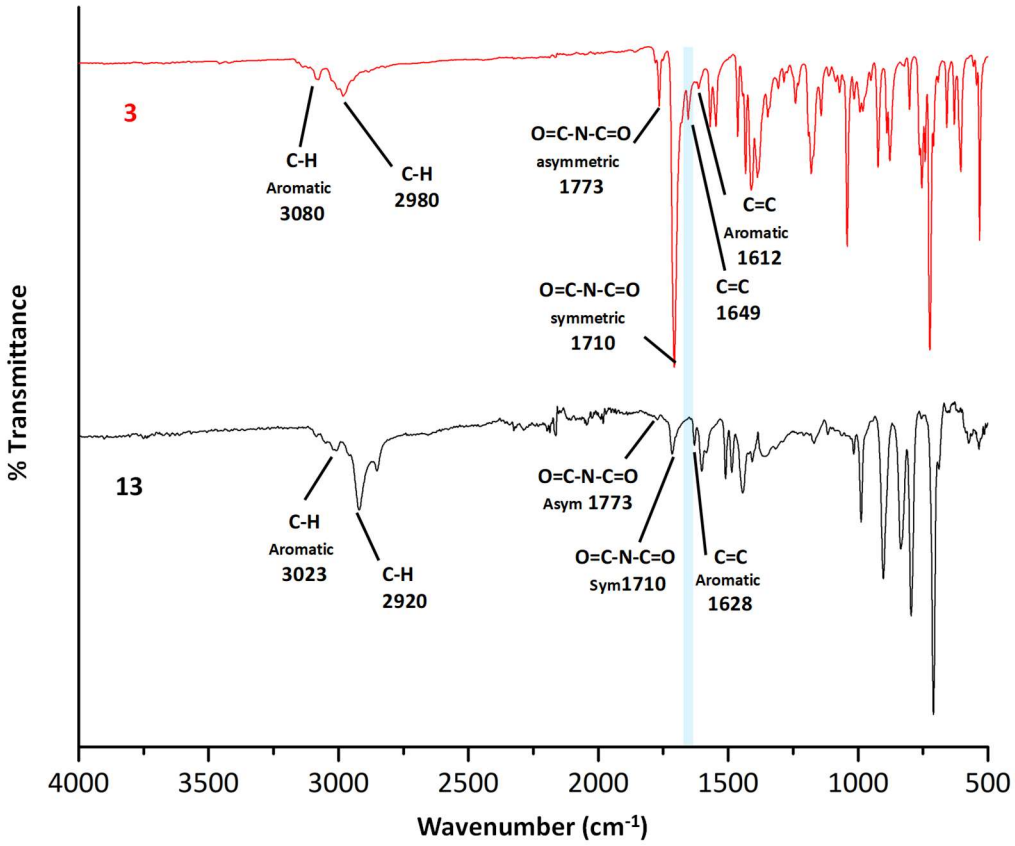

Figure S8. ATR-FTIR spectra of **3** (black trace) and *homo*-PIL-x1 (**13**, red trace).

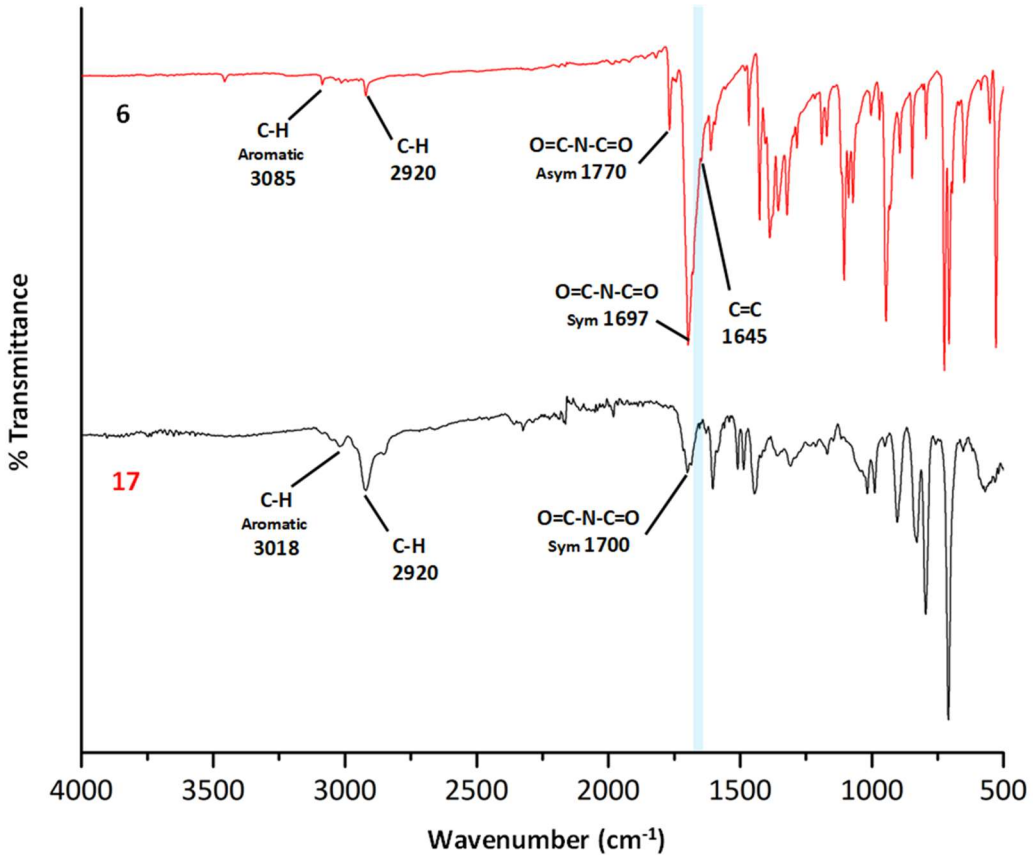

Figure S9. ATR-FTIR spectra of **6** (black trace) and *homo*-PAP (**17**, red trace).

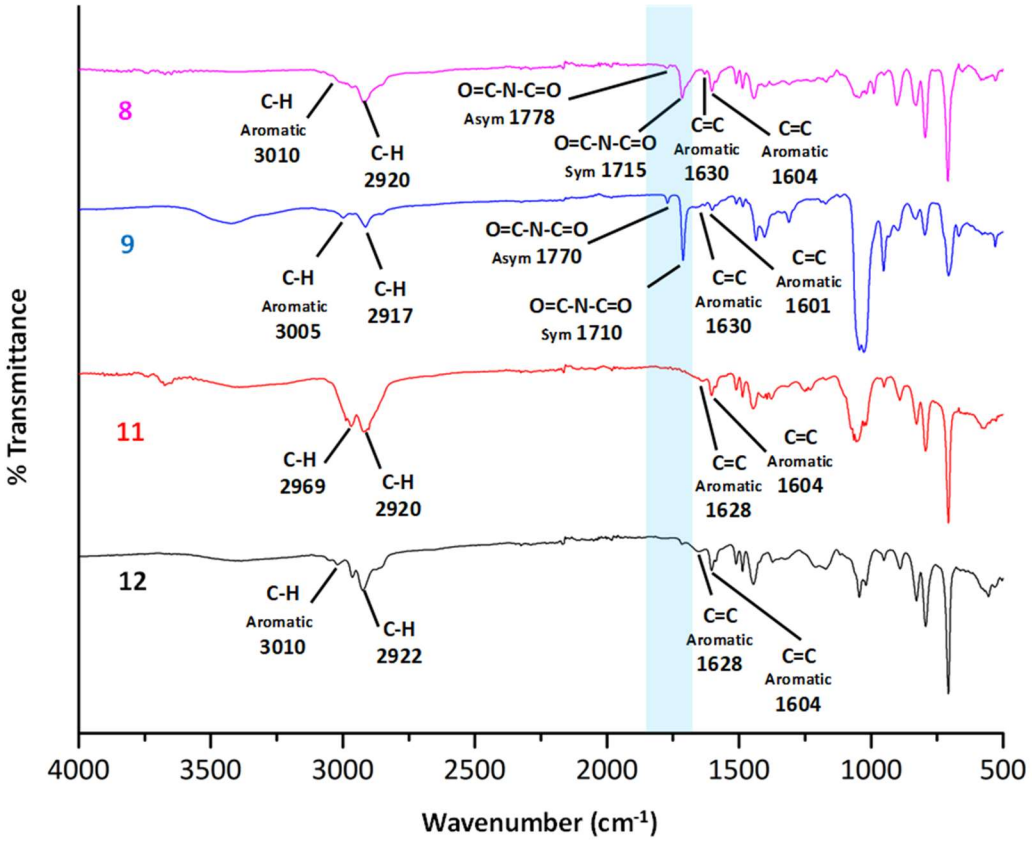

Figure S10. ATR-FTIR spectra of the prepared *co*-PILs: *co*-PIL-x2 (**8**, black trace), *co*-PIL-NH_2-x2 (**11**, red trace), *co*-PIL-x4 (**9**, blue trace) and *co*-PIL-NH_2-x4 (**12**, magenta trace).

Table S3. Specific surface area measurements for the synthesised PILs by multi-point BET.

Material	S_{BET} (m^2/g)
8	874
11	1378
9	994
12	1360
Poly(DVB)	239

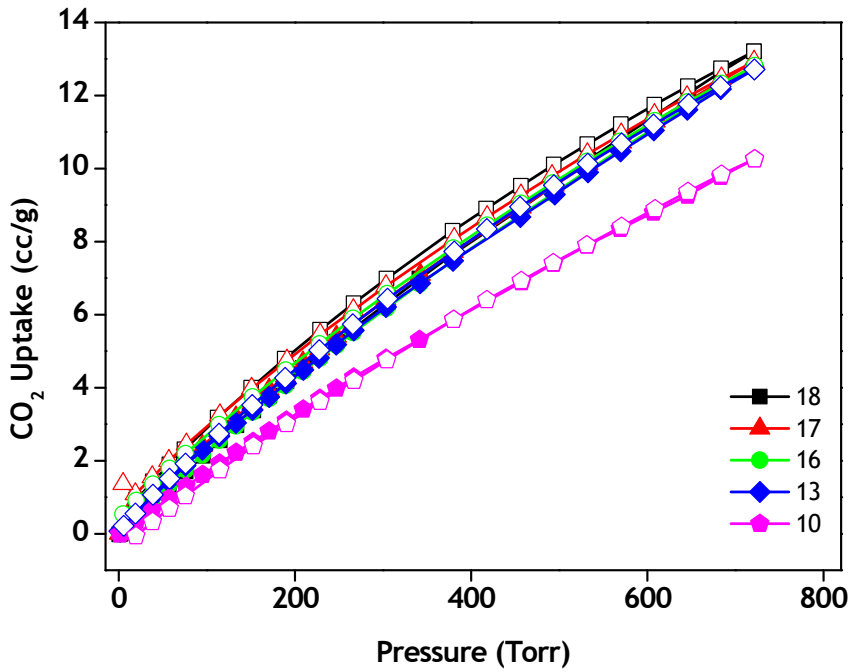

Figure S11. CO_2 sorption isotherms of the synthesised polymers (**10**, **13**, **16-18**) at 298 K. Filled and unfilled symbols show gas adsorption and desorption patterns, respectively.

Table S4. CO_2 capture efficiency data for vinylimidazolium-based PILs.

Substances	CO_2 uptake (mmol CO_2/g sorbent)
co-PIL-NH_2-x1 (**10**)	0.457
homo-PIL-x1 (**13**)	0.567
homo-PIL-NH_2-x1 (**16**)	0.572
homo-PAP (**17**)	0.577
homo-PAA (**18**)	0.589

Table S5. Frontier-orbital contour plots for the optimised geometries (at B3LYP/6-31G* level of theory) for the monomeric reactants, and the HOMO-LUMO energy gaps.

	HOMO	LUMO	$\Delta E_{(HOMO–LUMO)}$ / eV
3	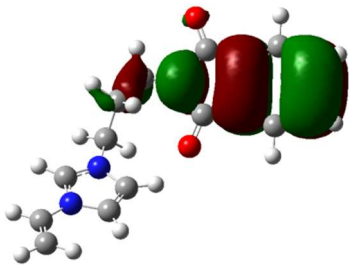	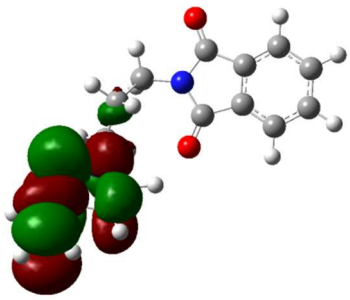	4.61

6	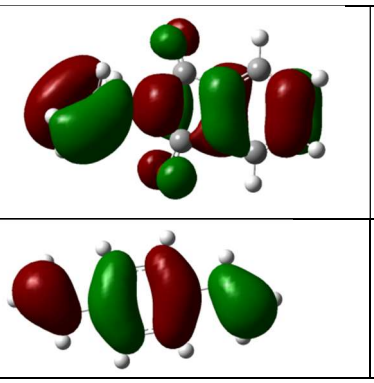	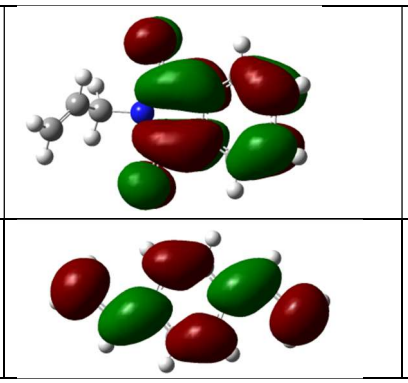	4.95
DVB			4.41

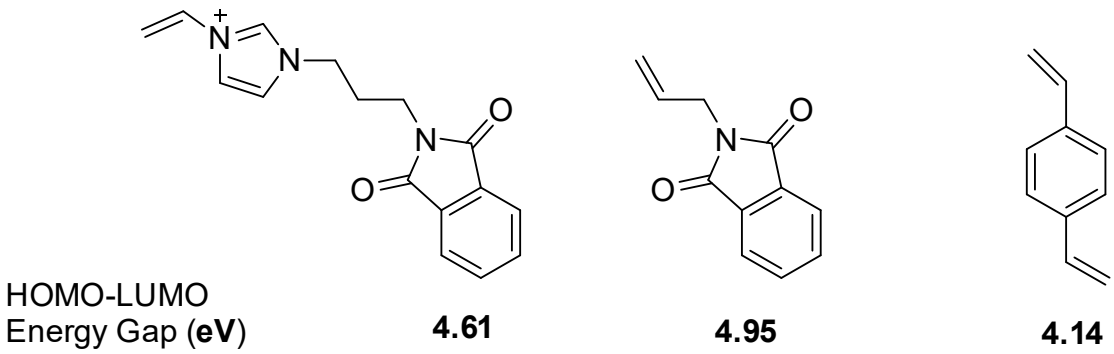

Figure S12. Calculated HOMO-LUMO gaps for the starting materials (at B3LYP/6-31G* in gas phase using Gaussian 09 program).

Table S6. Catalytic performance of various PILs for the cycloaddition of CO_2 versus PO, ECH and SO

Entry	Catalyst	Epoxide	*P* (bar)	T (°C)	Time (h)	Yield (%)	Selectivity (%)	Ref
1	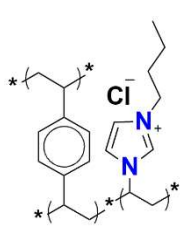 a	PO	60	110	6	97	--	20
		ECH			3	96		
2	 b	PO	60	110	6	75	--	20

3	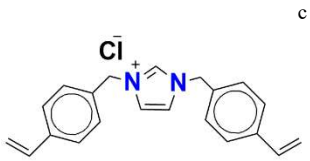 c	ECH	50	140	3	98	>99	21
4	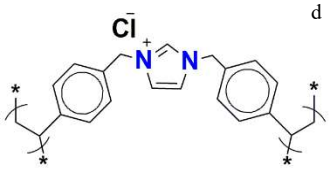 d	ECH	50	140	3	98	>99	21
5	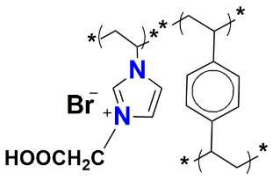 e	ECH	25	130	3	98	99	22
6	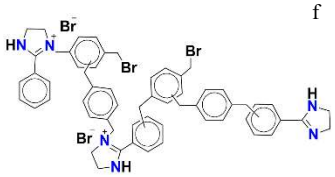 f	ECH	1	25	96	96	>99	23
7	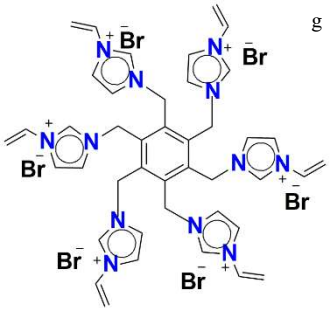 g	ECH	1	50	24	98	>99	6
8	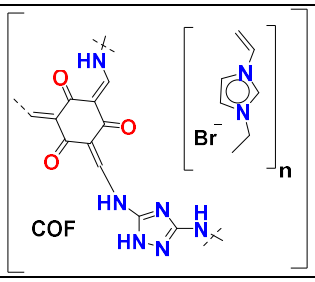 h	ECH	1	120	10	>99	99	24

9	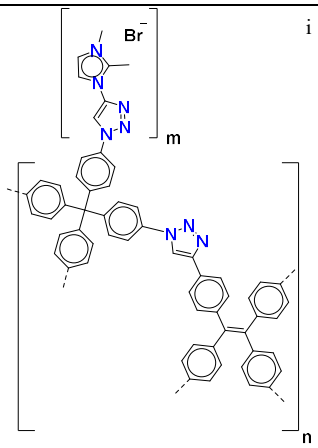 i	ECH	1	100	24	>99	>99	25
10	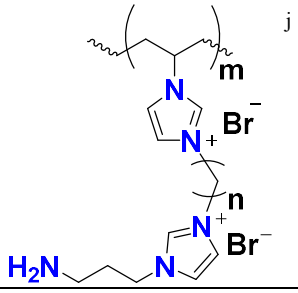 j	ECH	20	100	4	99	99	26
11	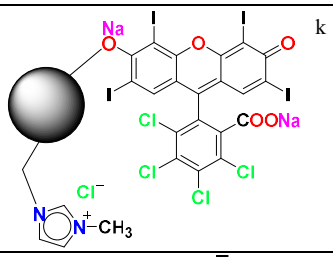 k	SO	10	100	5	93	-	27
12	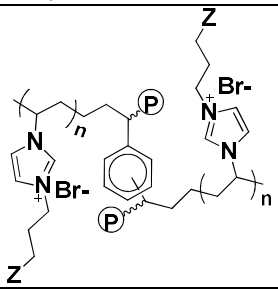	ECH	10	110	24	99	-	This Work

[a] Highly cross-linked polymer-supported IL; poly(3-butyl-1-vinylimidazolium chloride)(divinyl benzene). [b] Poly(3-butyl-1-vinylimidazolium chloride). [c] 1,3-bis(4-vinylbenzyl) imidazolium chloride. [d] Cross-linked poly(bis-1,3-vinylbenzyl) imidazolium chloride. [e] Cross-linked polymer- supported IL; poly(1-vinyl-3-carboxyethylimidazolium bromide)(divinylbenzene). [f] Hyper cross-linked poly(2-phenylimidazolinium bromide). [g] Poly(1,2,3,4,5,6-hexakis (methyl) benzene vinylimidazolium bromide); the shown chemical structure corresponds for the monomeric unit. [h] Imidazolium-based ionic polymer (ImIP/Host)@ (COF/guest). [i] Polymer from tetrakis(4-azidophenyl)methane, 1,1,2,2-tetrakis(4- ethynylphenyl)ethane and 1,2-Dimethyl-3-(prop-2-ynyl)-1H-imidazol-3-ium bromide. [j] Poly bis-imidazolium ionic liquids. [k] Rose Bengal (RB) immobilised onto supported ionic liquid-like phases.

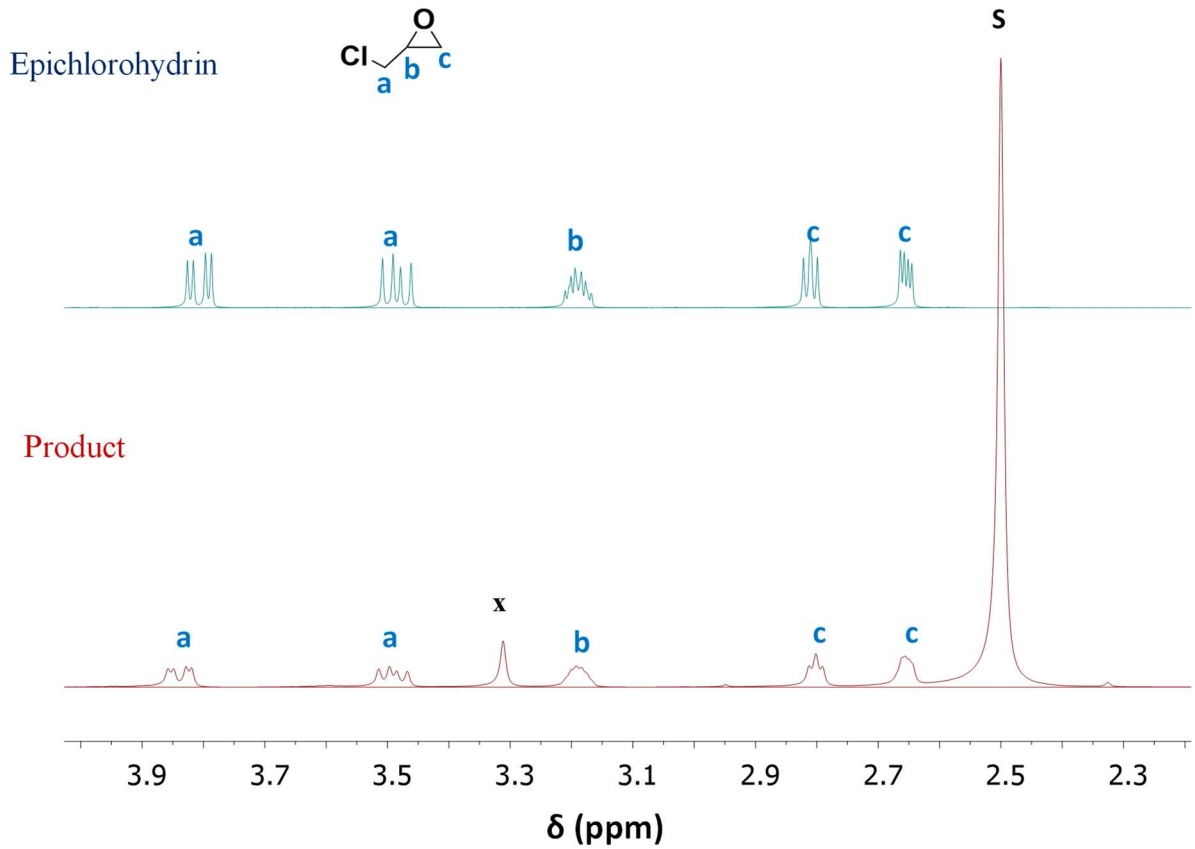

Figure S13. The ^{1}H NMR spectra of the ECH with 0% conversion of its corresponding CC in DMSO-d_6; **S**: Solvent; **x**: H_2O, catalyzed by poly(DVB) (Entry 1, Table 2).

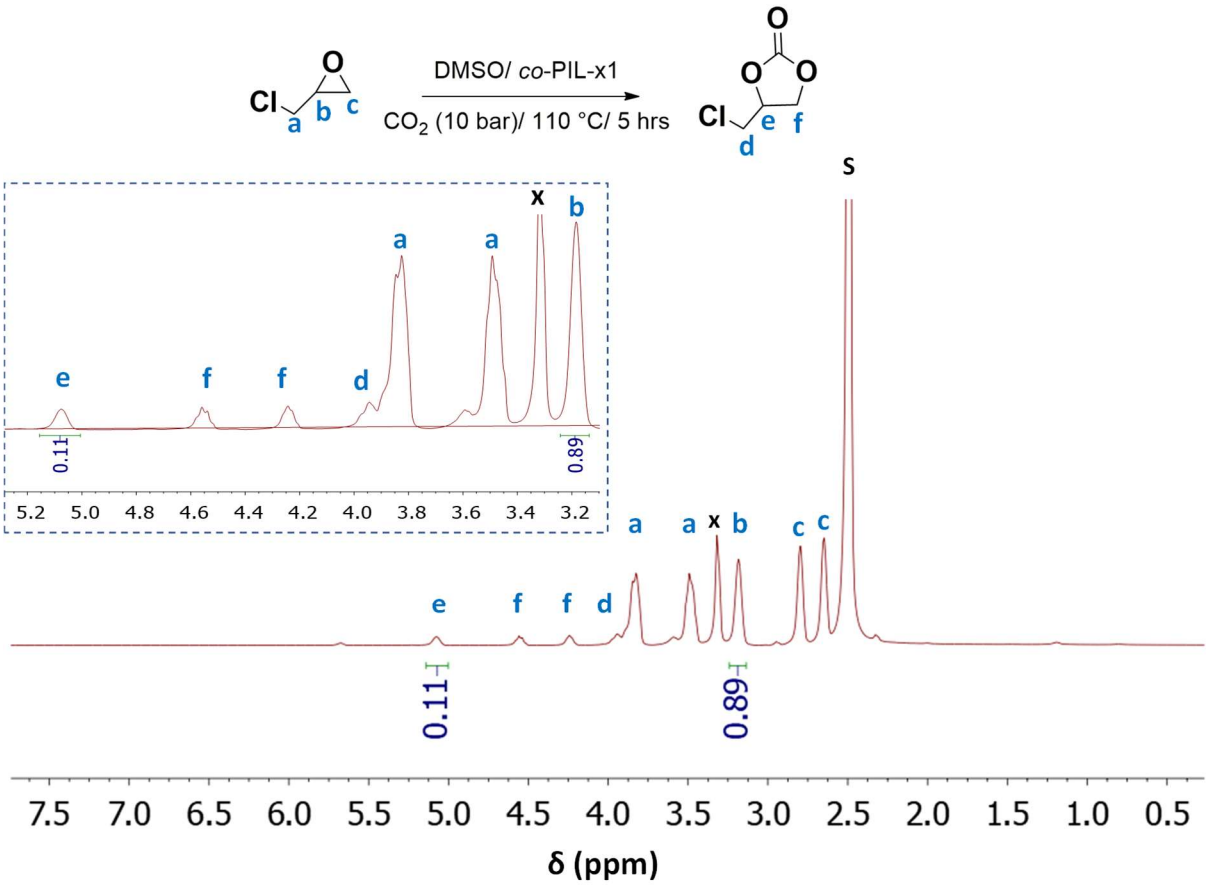

Figure S14. The ^{1}H NMR spectrum of epichlorohydrin carbonate in DMSO-d_6; **S**: Solvent; **x**: H_2O, catalyzed by *co*-PIL-x1 at 5 h with a conversion of 11% (Entry 2, Table 2).

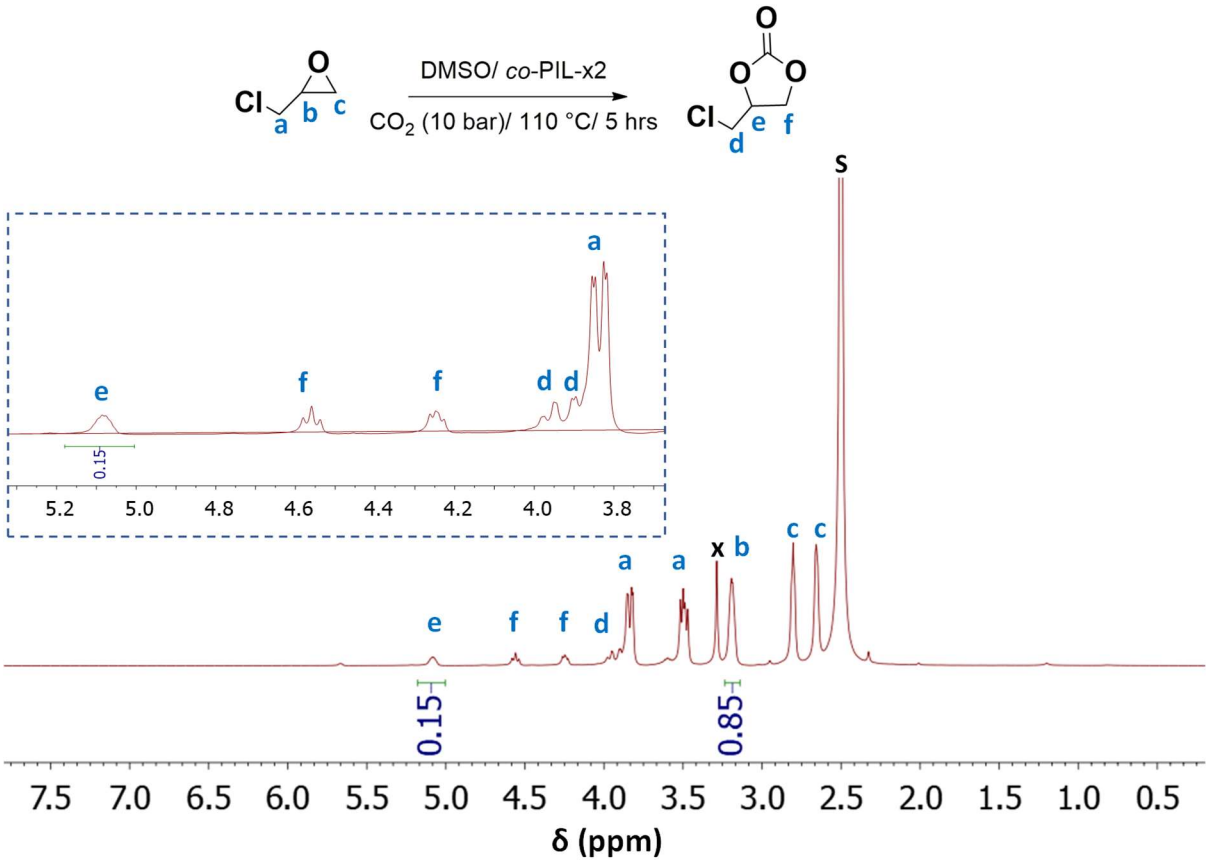

Figure S15. The ^{1}H NMR spectrum of epichlorohydrin carbonate in DMSO-d_6; **S**: Solvent; **x**: H_2O catalyzed by *co*-PIL-x2 at 5 h with a conversion of 15%. (Entry 3, Table 2).

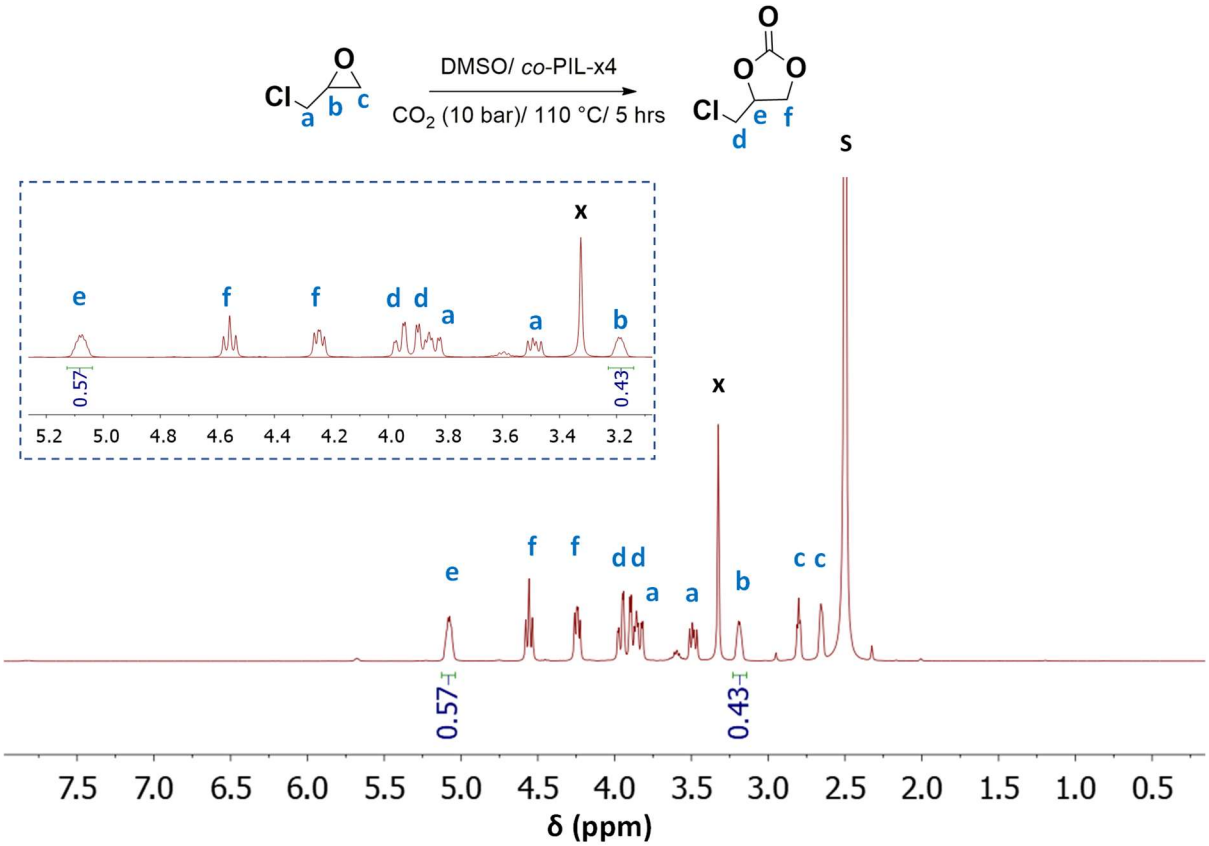

Figure S16. The ^{1}H NMR spectra of epichlorohydrin carbonate in DMSO-d_6; **S**: Solvent; **x**: H_2O catalyzed by *co*-PIL-x4 at 5 h with a conversion of 57% (Entry 4, Table 2).

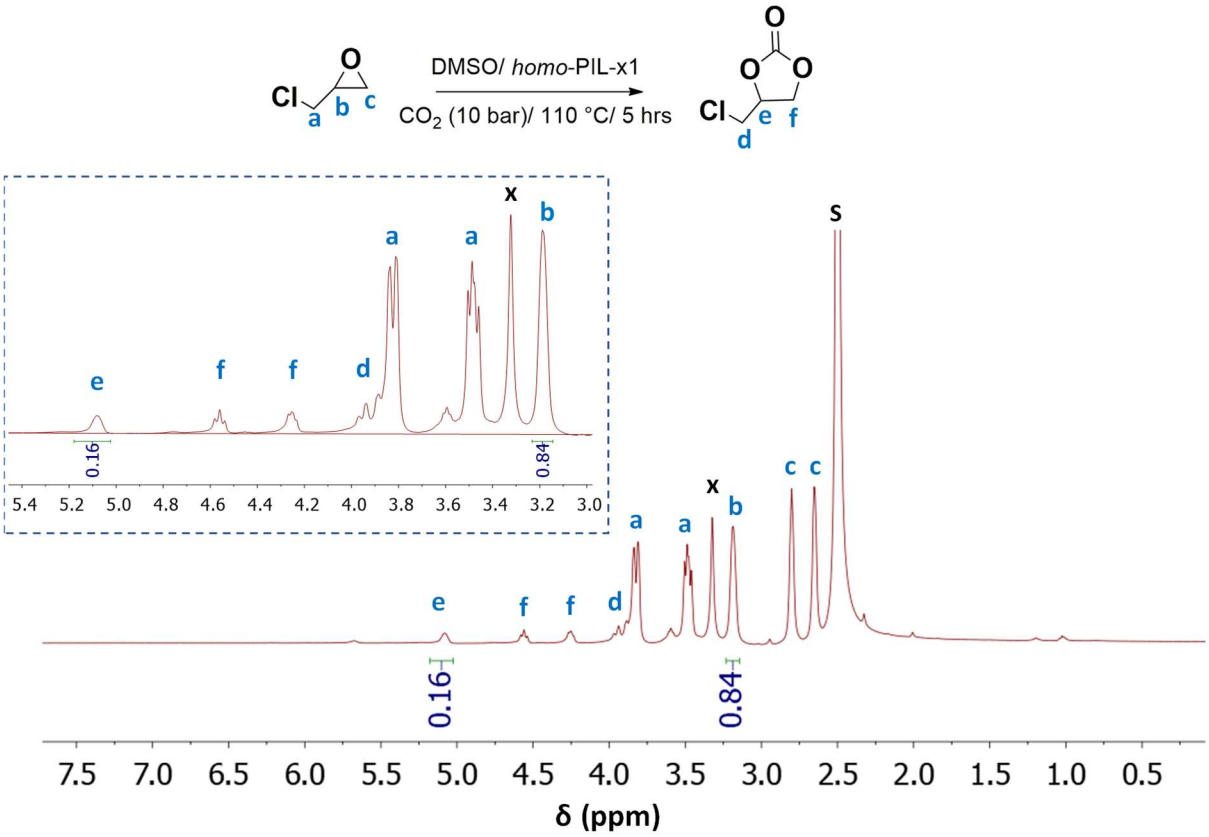

Figure S17. The ^{1}H NMR spectrum of epichlorohydrin carbonate in DMSO-d_6; **S**: Solvent; **x**: H_2O catalyzed by *homo*-PIL-x1 at 5 h with a conversion of 16% (Entry 5, Table 2).

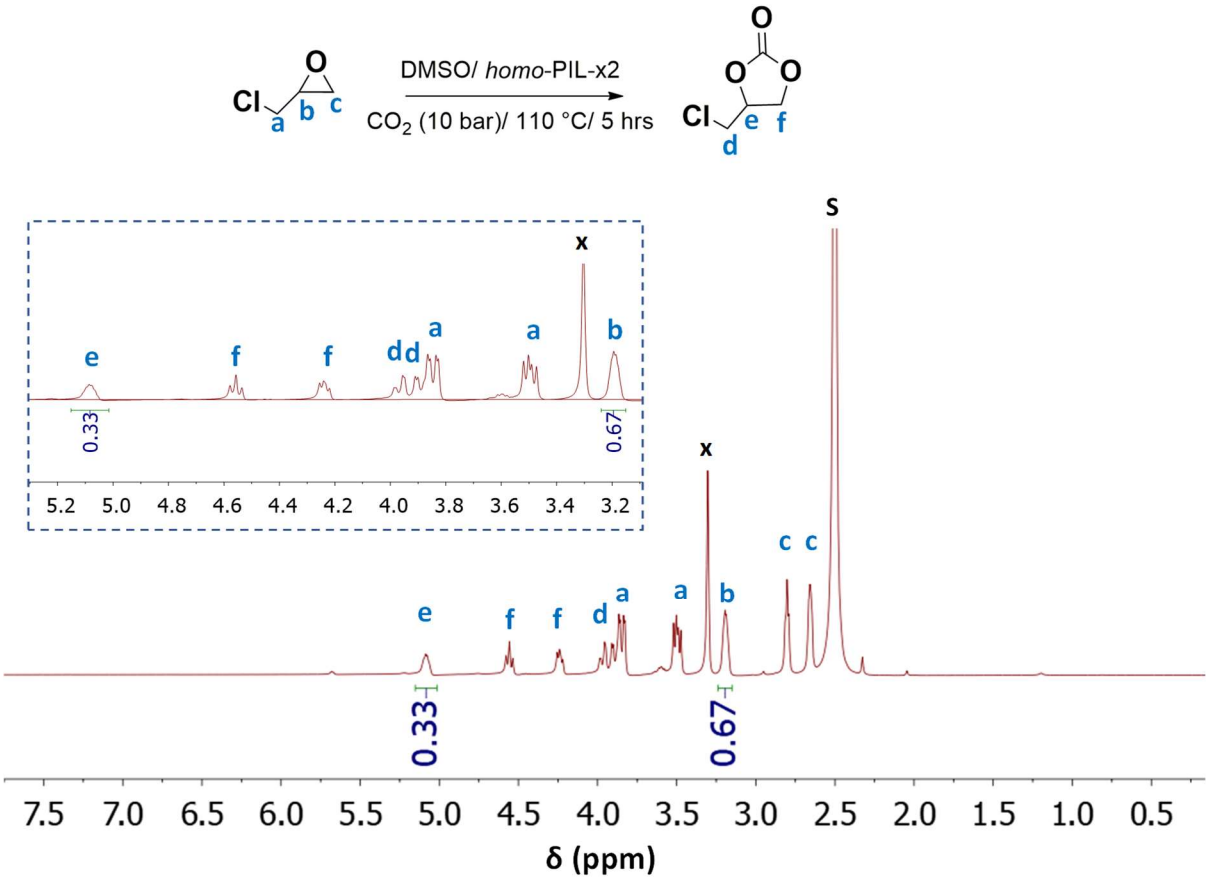

Figure S18. The ^{1}H NMR spectrum of epichlorohydrin carbonate in DMSO-d_6; **S**: Solvent; **x**: H_2O catalyzed by *homo*-PIL-x2 at 5 h with a conversion of 33% (Entry 6, Table 2).

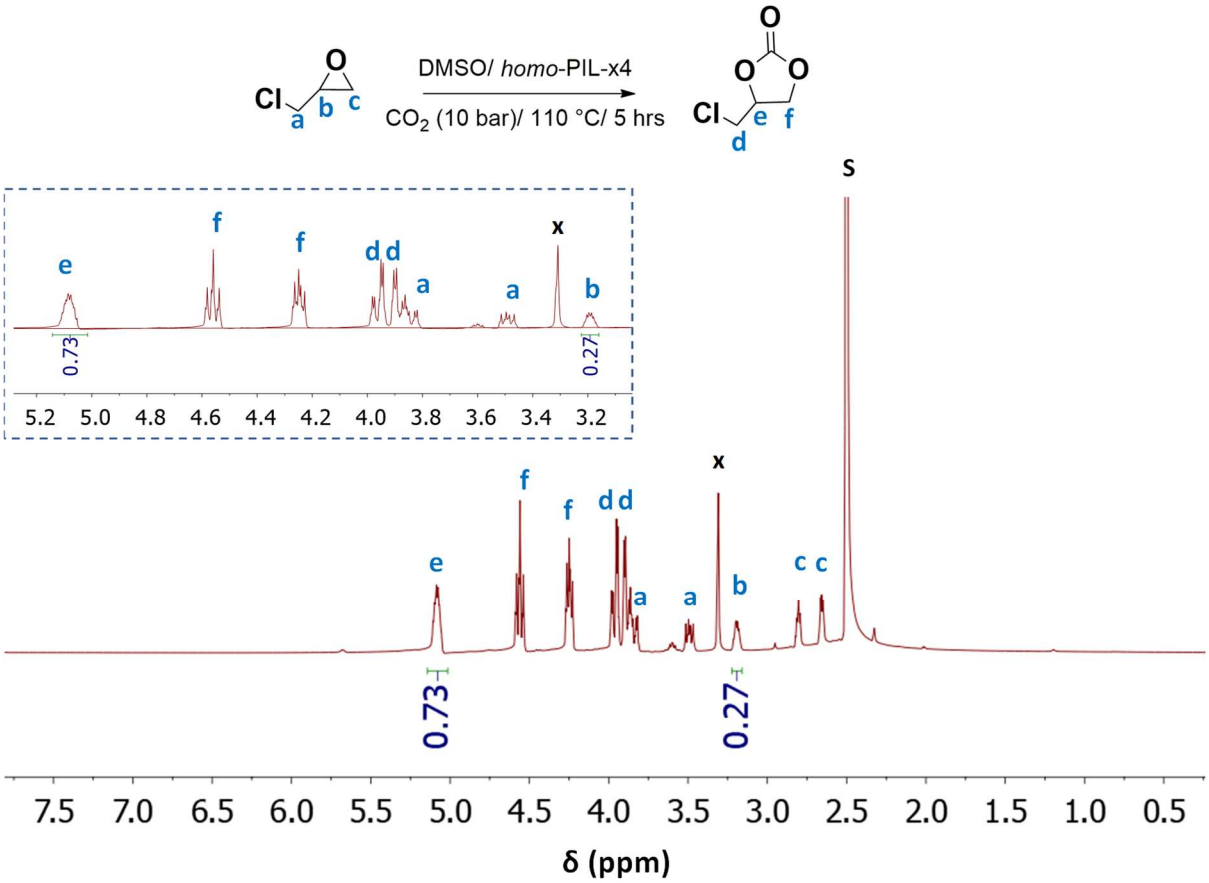

Figure S19. The ^{1}H NMR spectrum of epichlorohydrin carbonate in DMSO-d_6; **S**: Solvent; **x**: H_2O catalyzed by *homo*-PIL-x4 at 5 h with a conversion of 73% (Entry 6, Table 2).

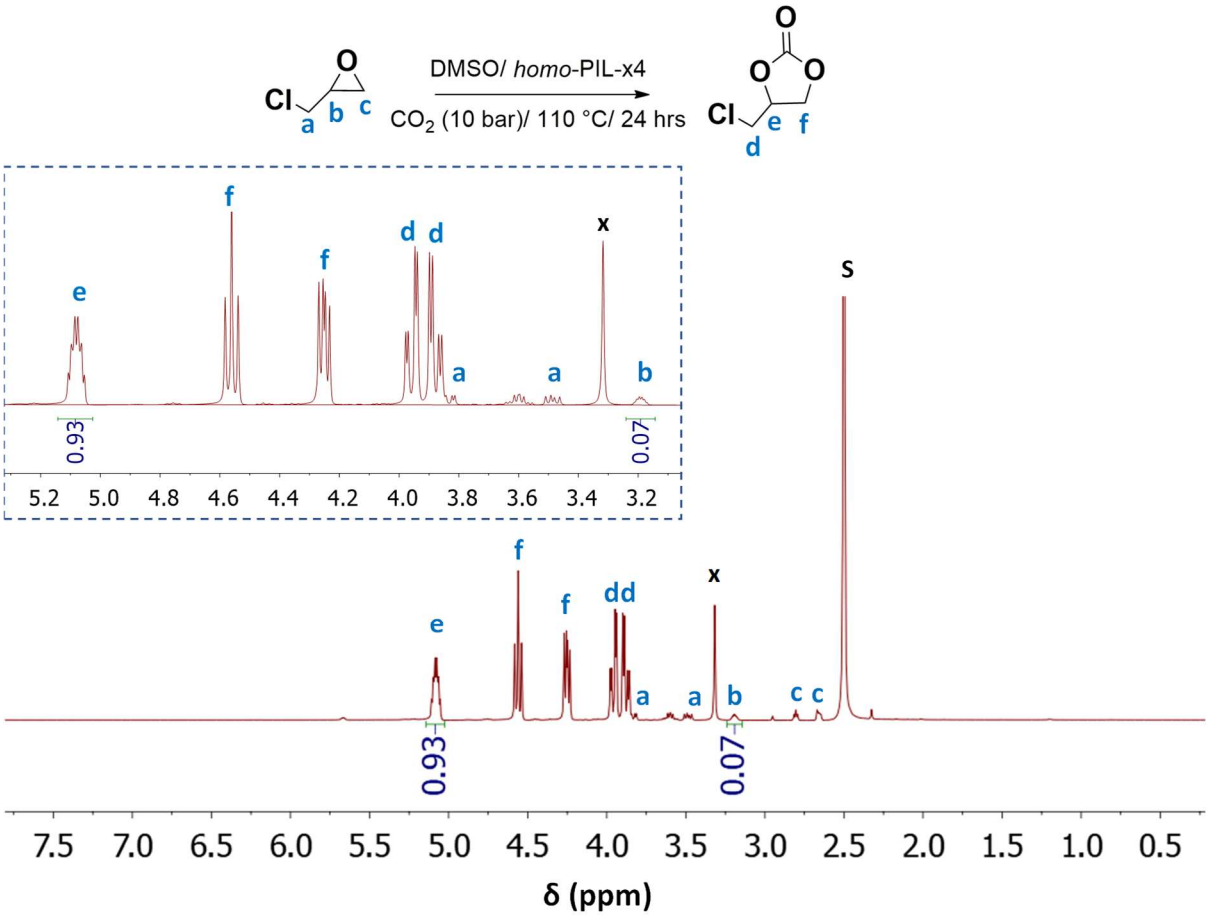

Figure S20. The ^{1}H NMR spectrum of the epichlorohydrin carbonate in DMSO-d_6; **S**: Solvent; **x**: H_2O catalyzed by *homo*-PIL-x4 at 24 h with a conversion of 93% (Entry 8, Table).

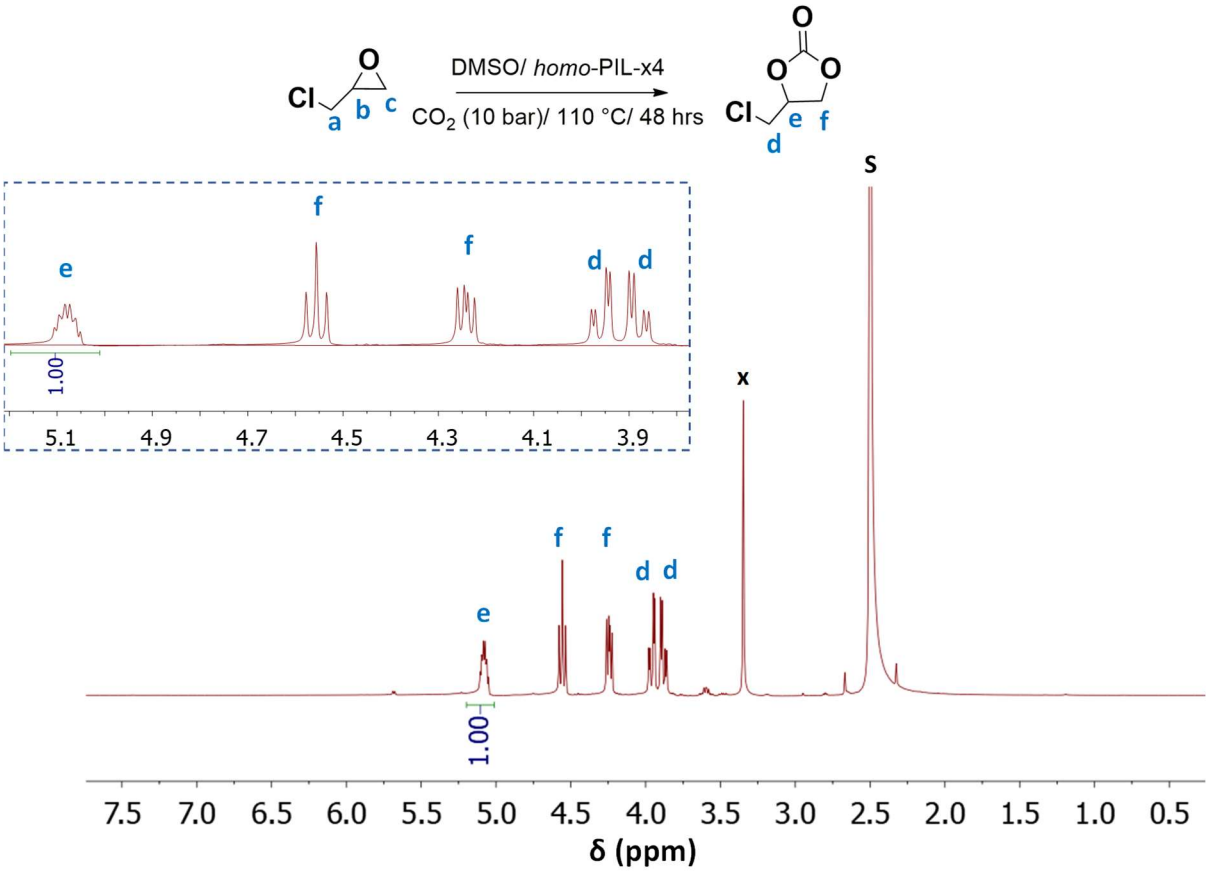

Figure S21. The ^{1}H NMR spectrum of the epichlorohydrin carbonate in DMSO-d_6; **S**: Solvent; **x**: H_2O catalyzed by *homo*-PIL-x4 at 48 h with a full conversion (Entry 9, Table 2).

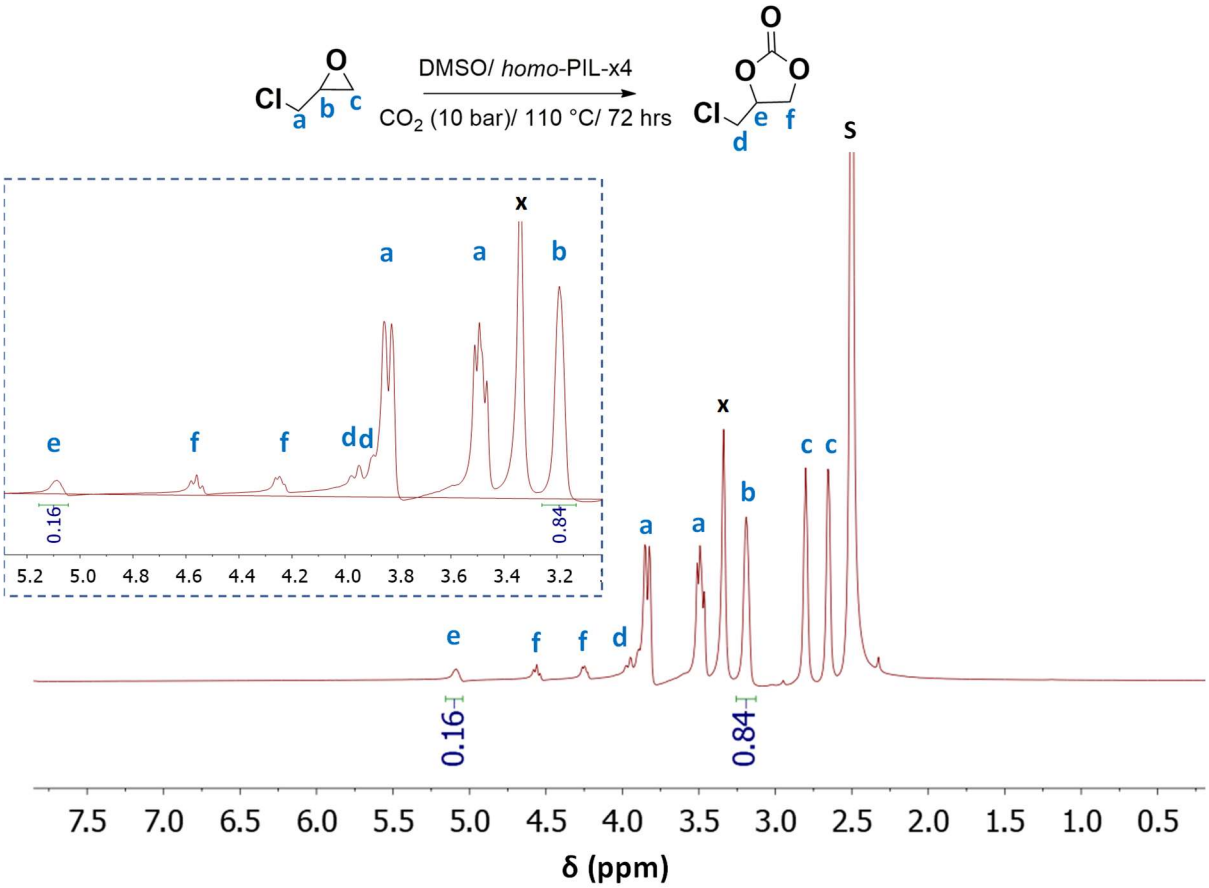

Figure S22. The ^{1}H NMR spectrum of the epichlorohydrin carbonate in DMSO-d_6; **S**: Solvent; **x**: H_2O catalyzed by *homo*-PIL-x4 at P_{CO2} (1 atm)/ T (20 °C) for 72 h with a conversion of 16% (Entry 10, Table 2).

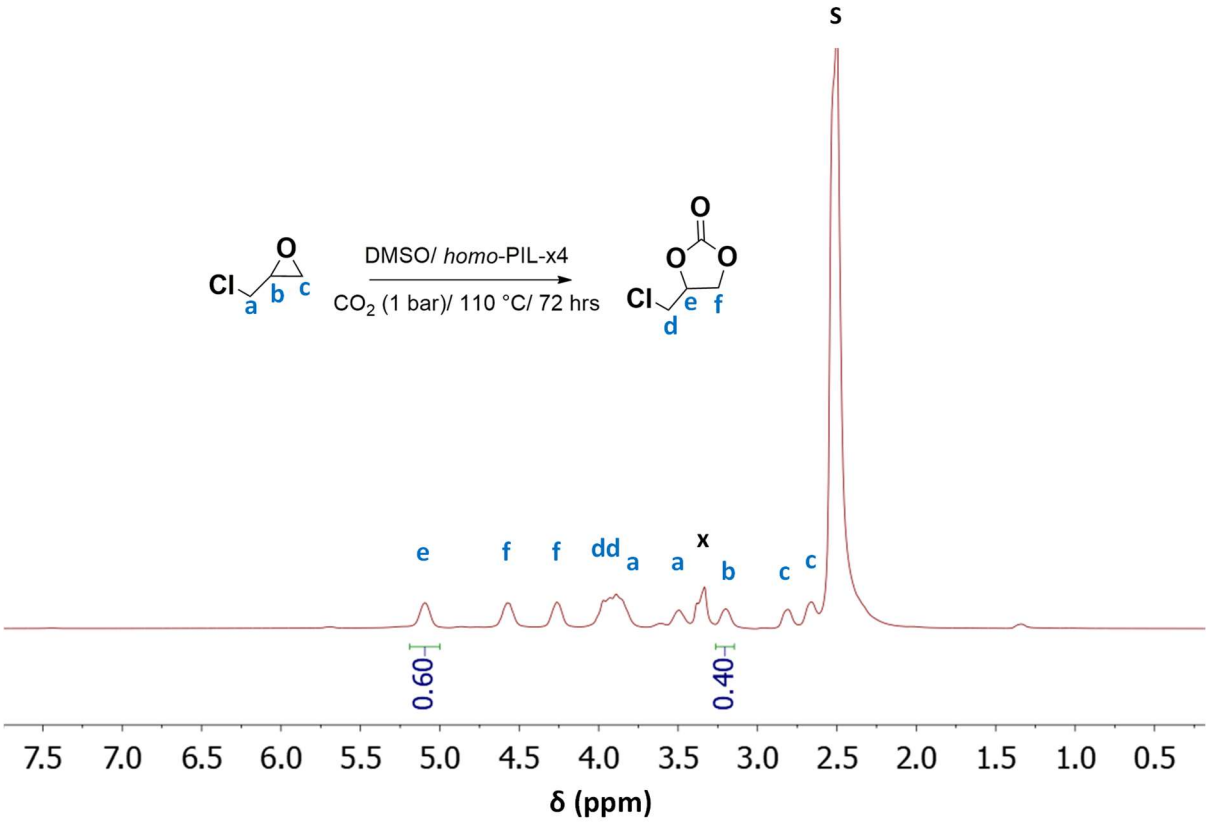

Figure S23. The ^{1}H NMR spectrum of the epichlorohydrin carbonate in DMSO-d_6; **S**: Solvent; **x**: H_2O catalyzed by *homo*-PIL-x4 at P_{CO2} (1 bar)/ T (110 °C) for 72 h with a conversion of 60% (Entry 11, Table 2).

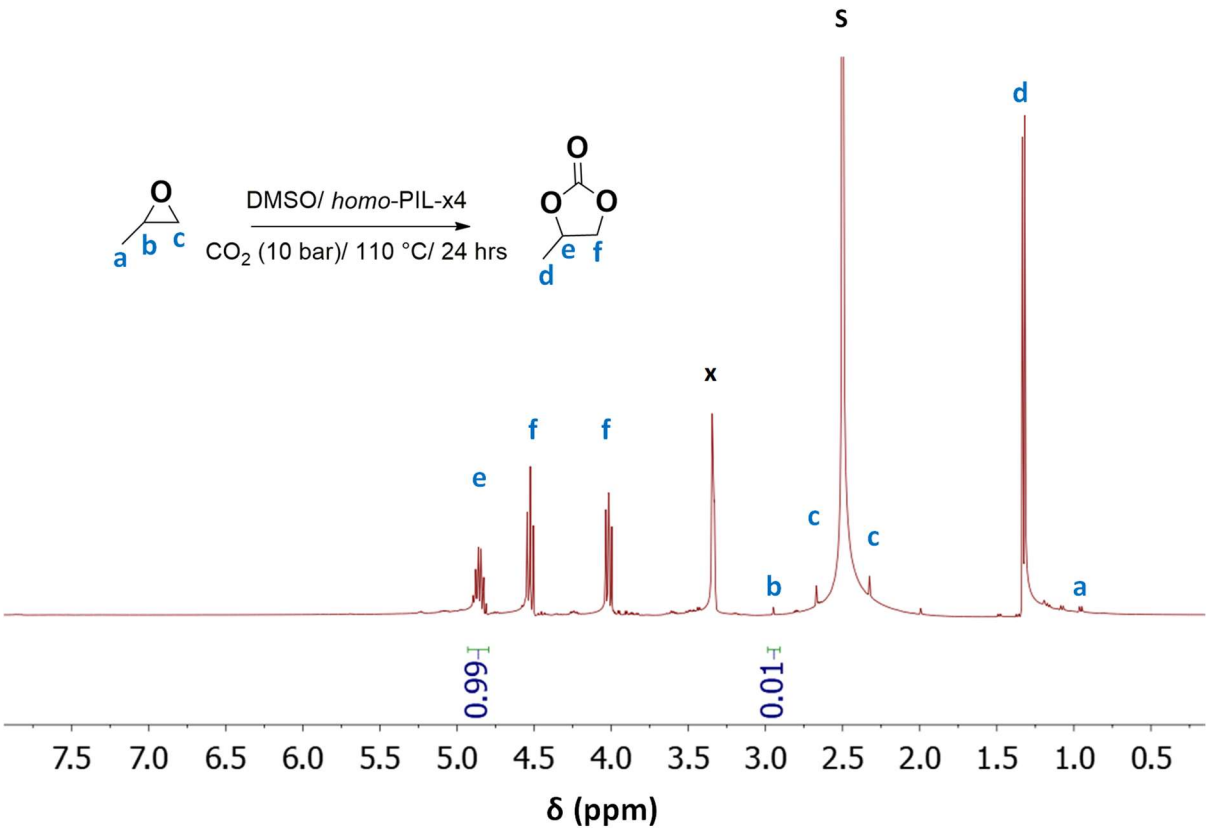

Figure S24.The ^{1}H NMR spectrum of the propylene carbonate in DMSO-d_6; **S**: Solvent; **x**: H_2O catalyzed by *homo*-PIL-x4 at 24 h with a conversion of 99% (Entry 1, Table 3).

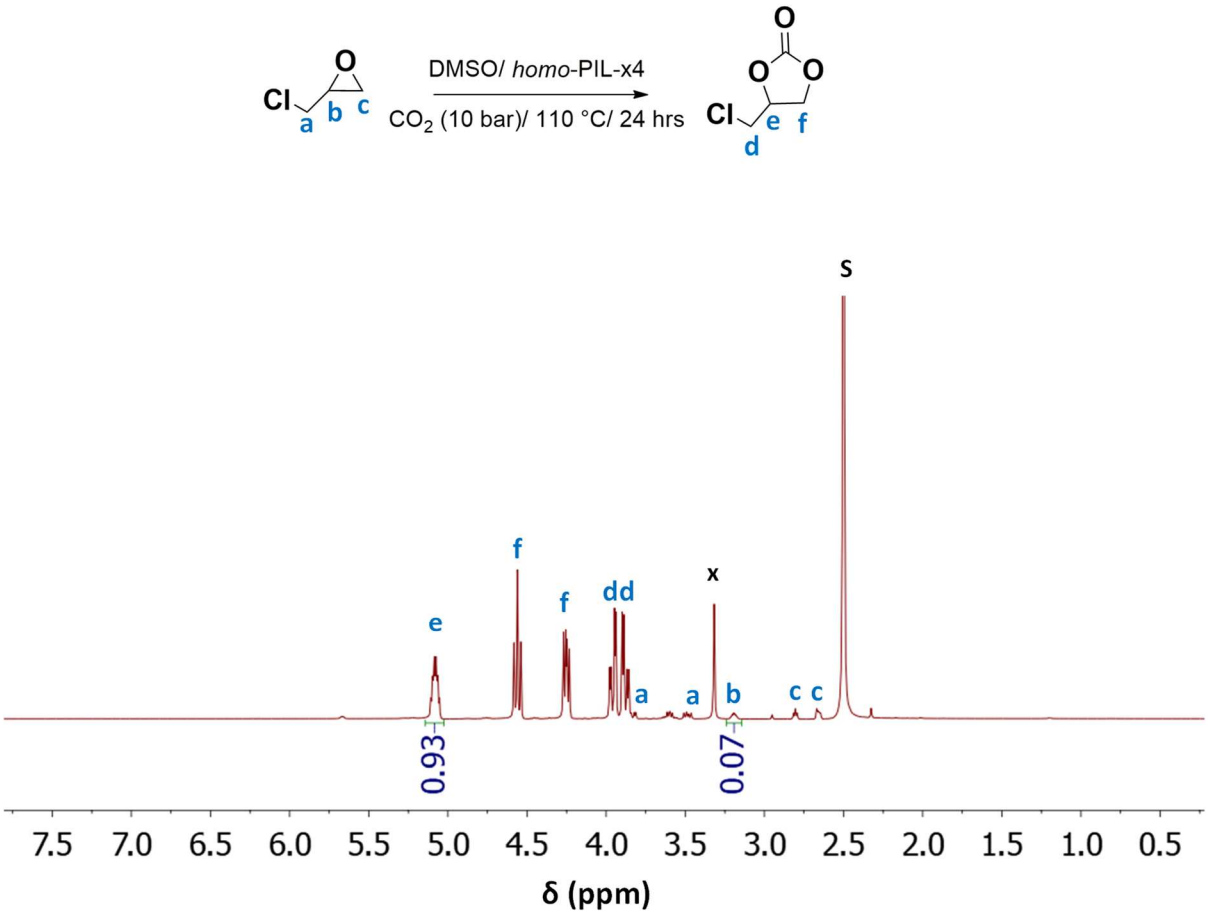

Figure S25. The ^{1}H NMR spectrum of the epichlorohyrin carbonate in DMSO-d_6; **S**: Solvent; **x**: H_2O, catalyzed by *homo*-PIL-x4 at 24 h with a conversion of 92 % (Entry 2, Table 3).

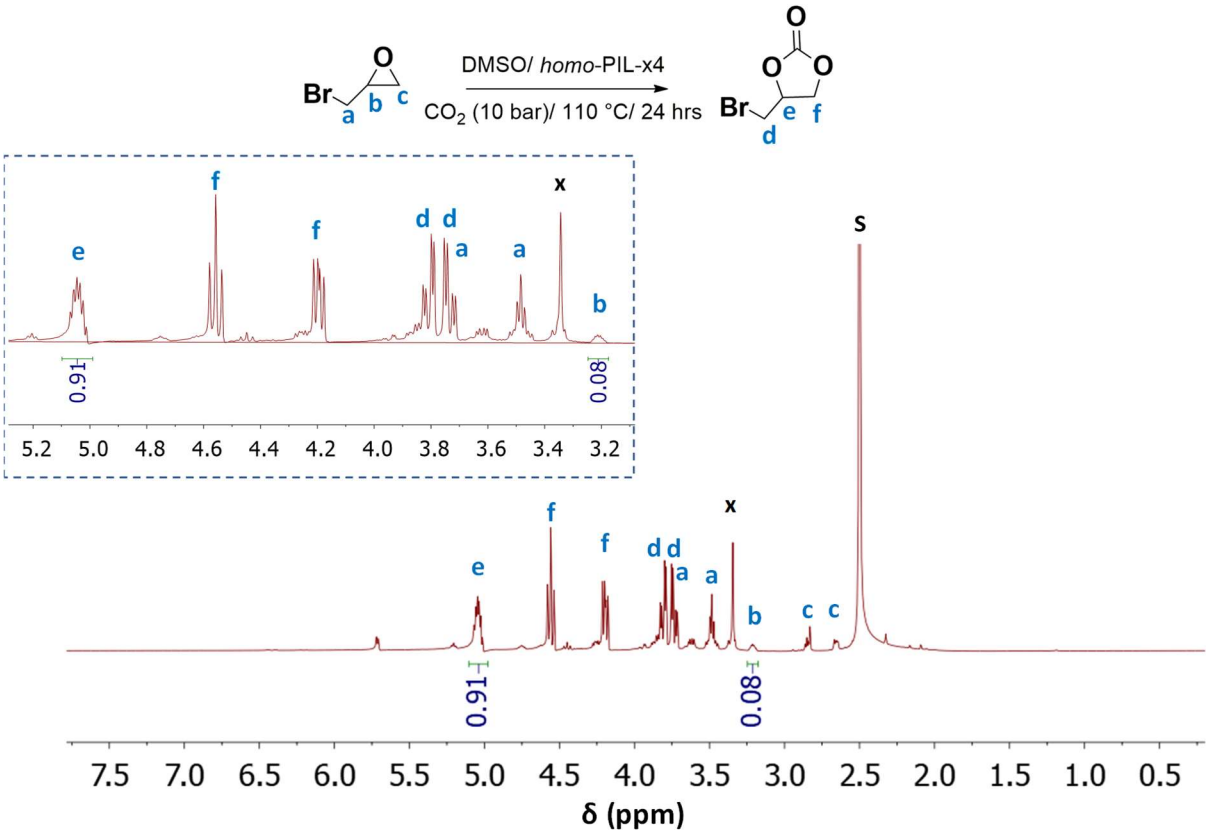

Figure S26. The ^{1}H NMR spectrum of the epibromohydrin carbonate in DMSO-d_6; **S**: Solvent; **x**: H_2O catalyzed by *homo*-PIL-x4 at P_{CO2} (1 bar)/ T (110 °C) for 24 h with a conversion of 91% (Entry 3, Table 3).

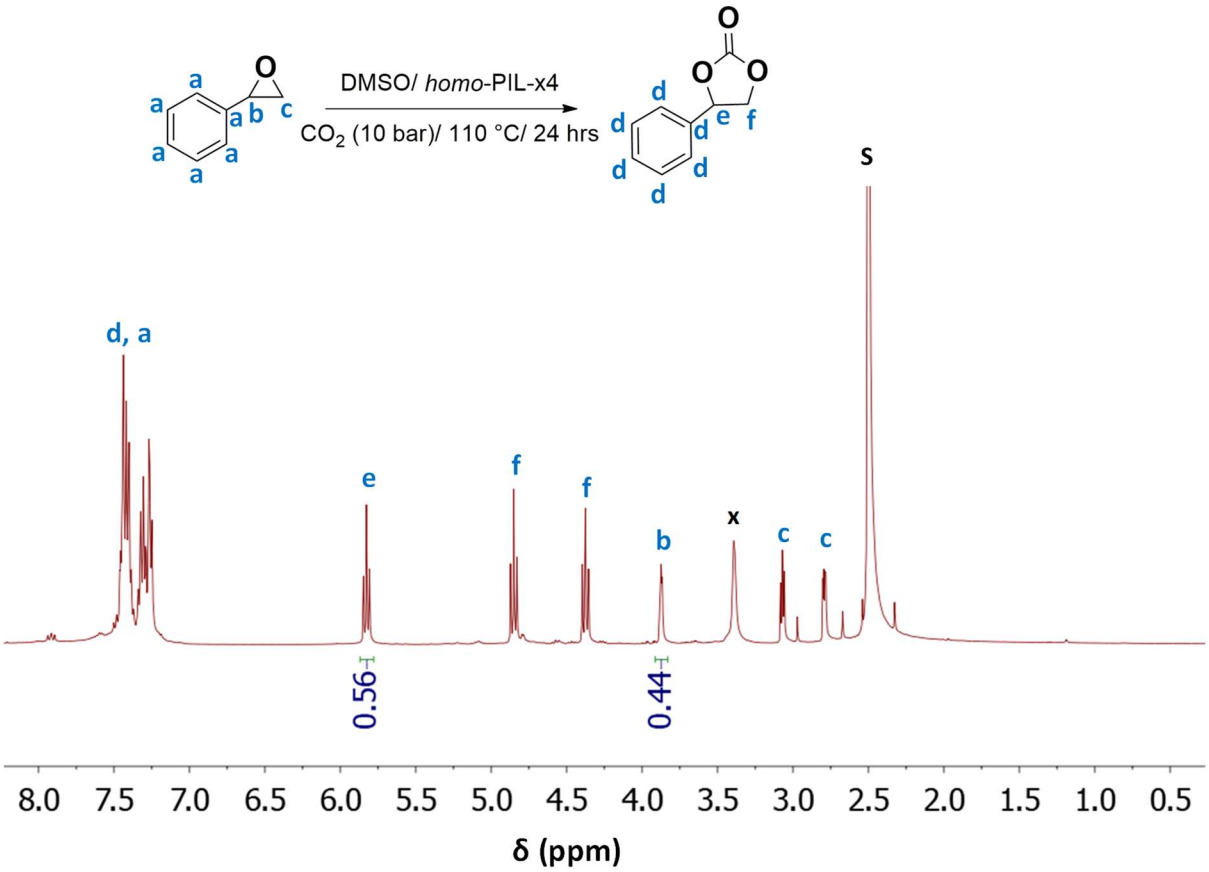

Figure S27. The ^{1}H NMR spectrum of the styrene carbonate in DMSO-d_6; **S**: Solvent; **x**: H_2O catalyzed by *homo*-PIL-x4 at 5h with a conversion 56% (Entry 4, Table 3).

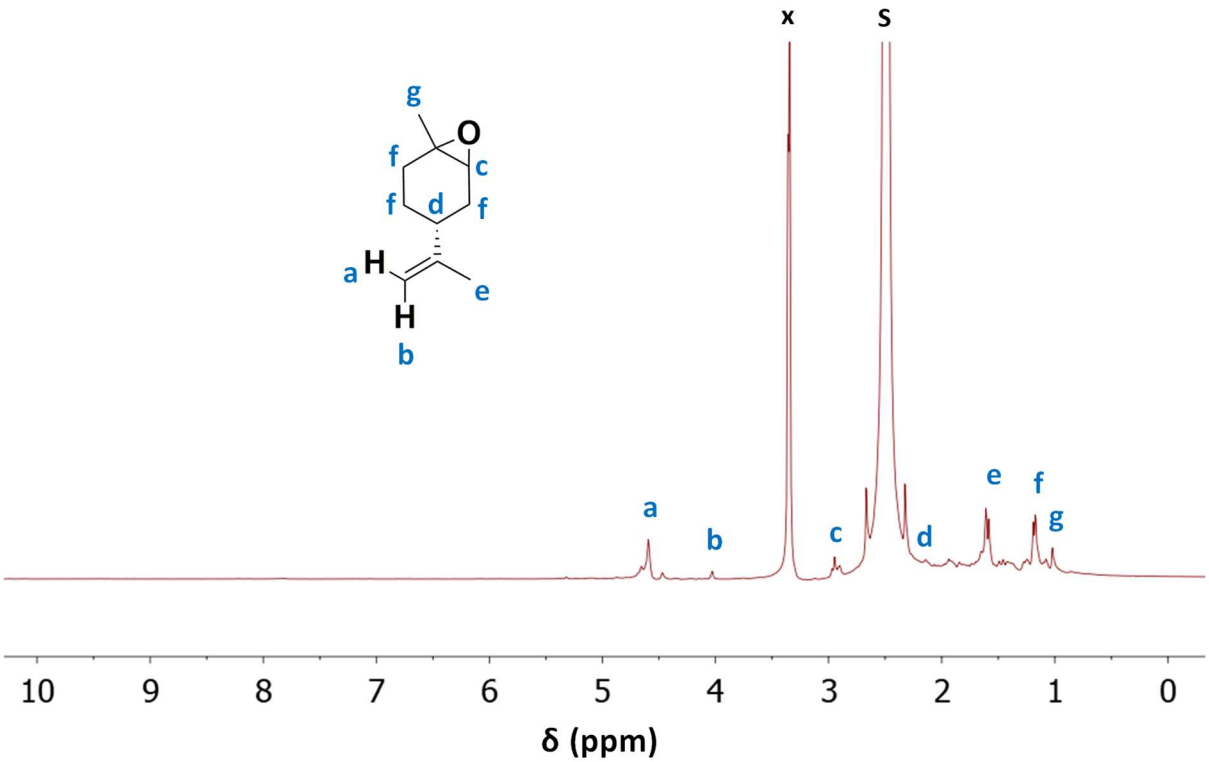

Figure S28. The ^{1}H NMR spectrum of the crude reaction in DMSO-d_6; **S**: Solvent; **x**: H_2O, catalyzed by *homo*-PIL-x4 at 24 h (Entry 5, Table 3).

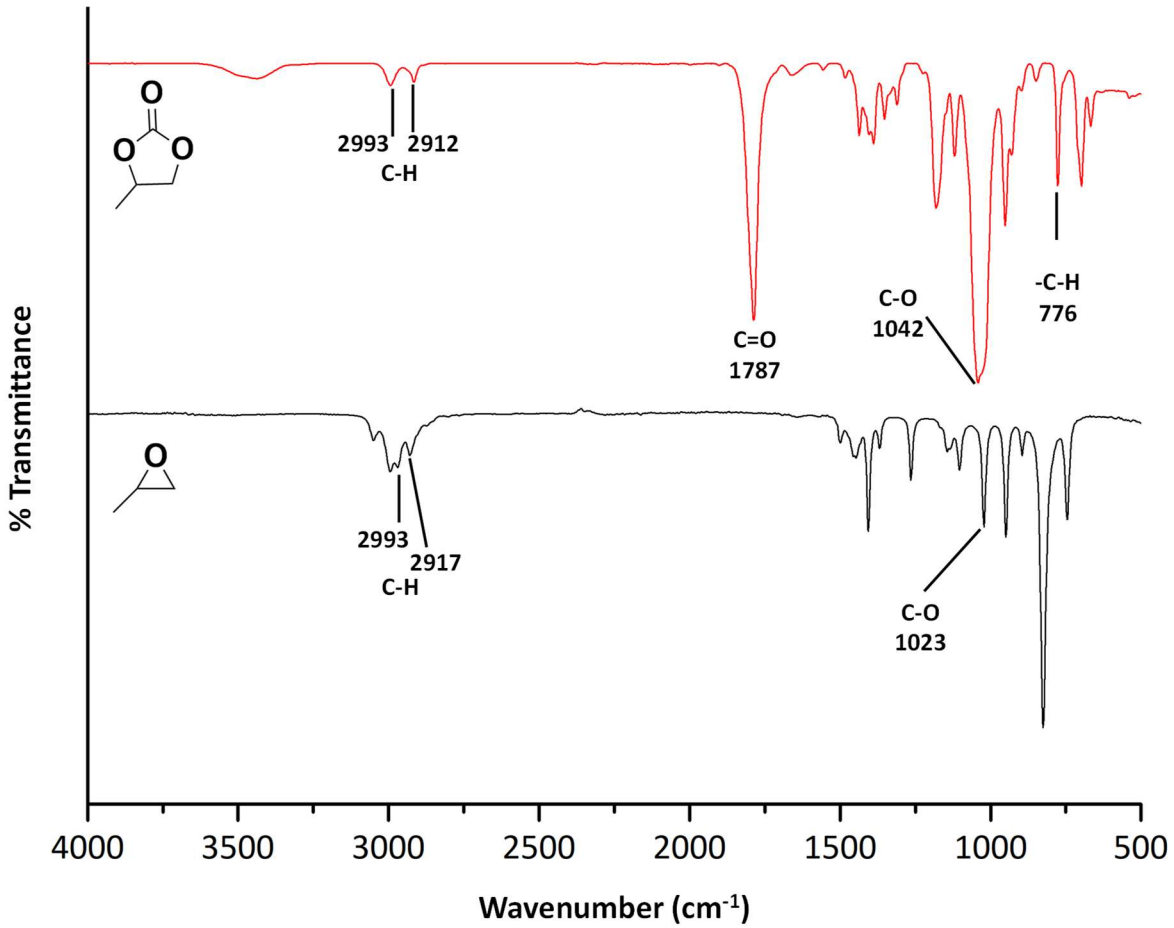

Figure S29. ATR-FTIR spectra of the propylene oxide (black trace) and propylene carbonate (red trace) (Entry 1, Table 3).

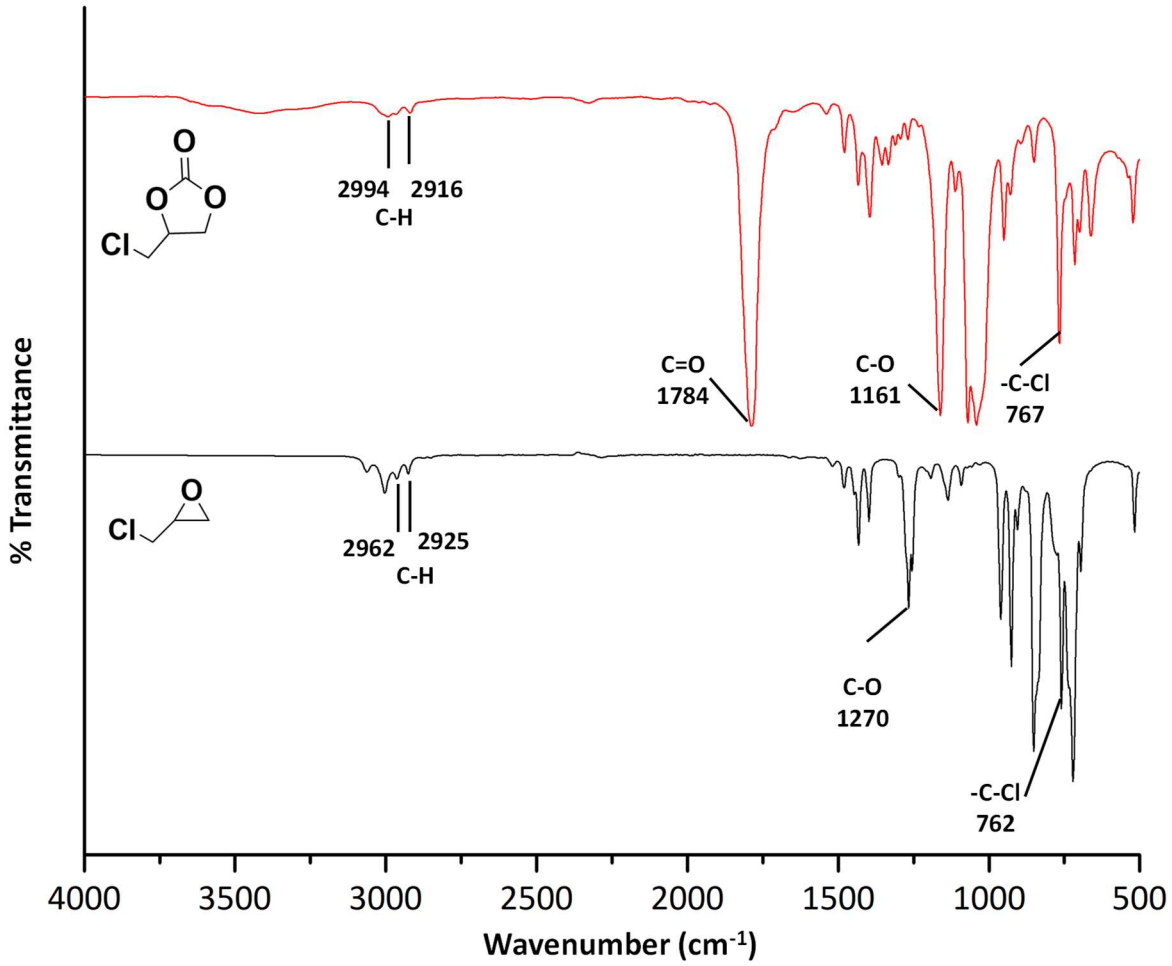

Figure S30. ATR-FTIR spectra of the epichlorohydrin (black trace) and epichlorohydrin carbonate (red trace) (Entry 2, Table 3).

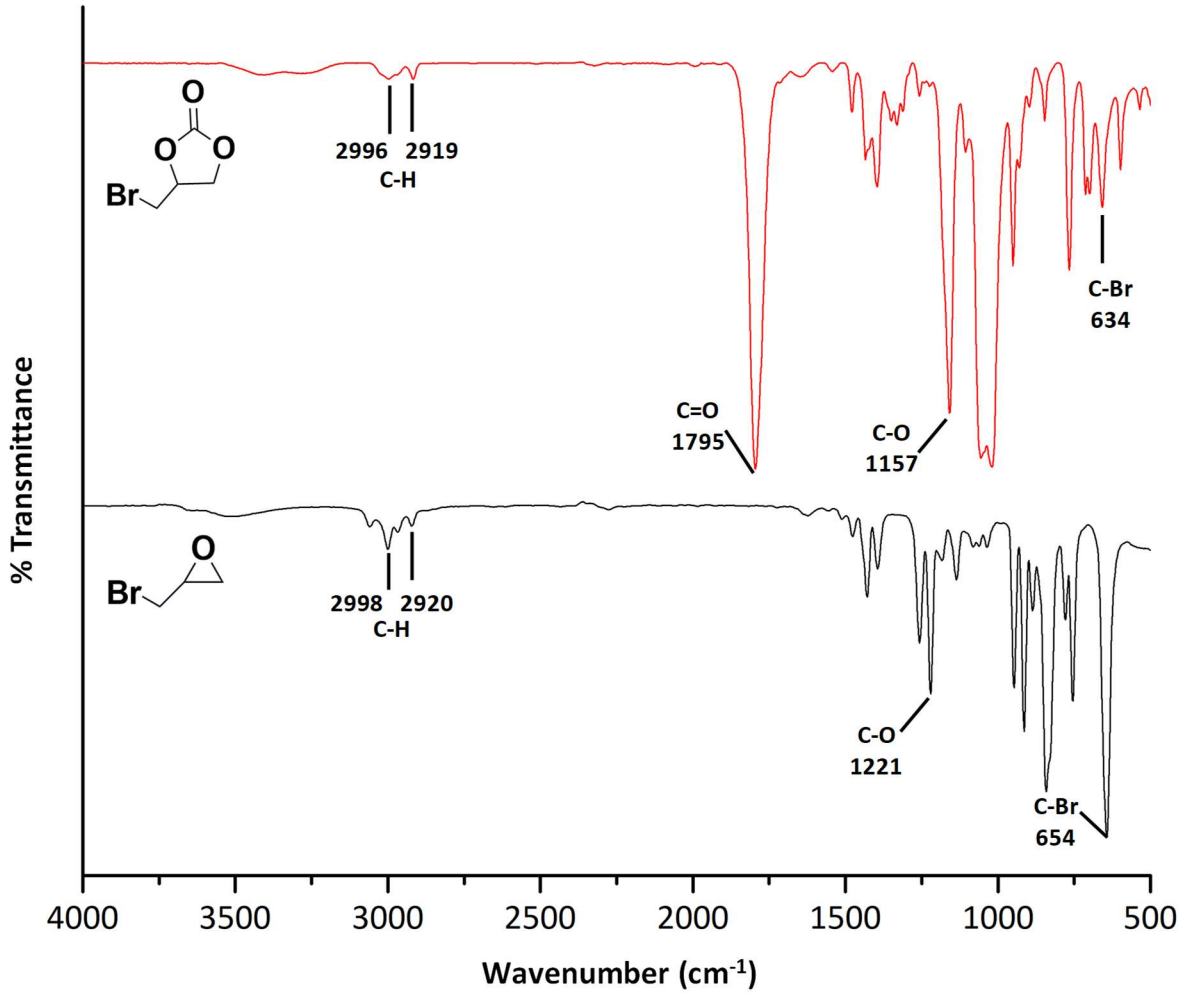

Figure S31. ATR-FTIR spectra of the epibromohydrin (black trace) and epibromohydrin carbonate (red trace) (Entry 3, Table 3).

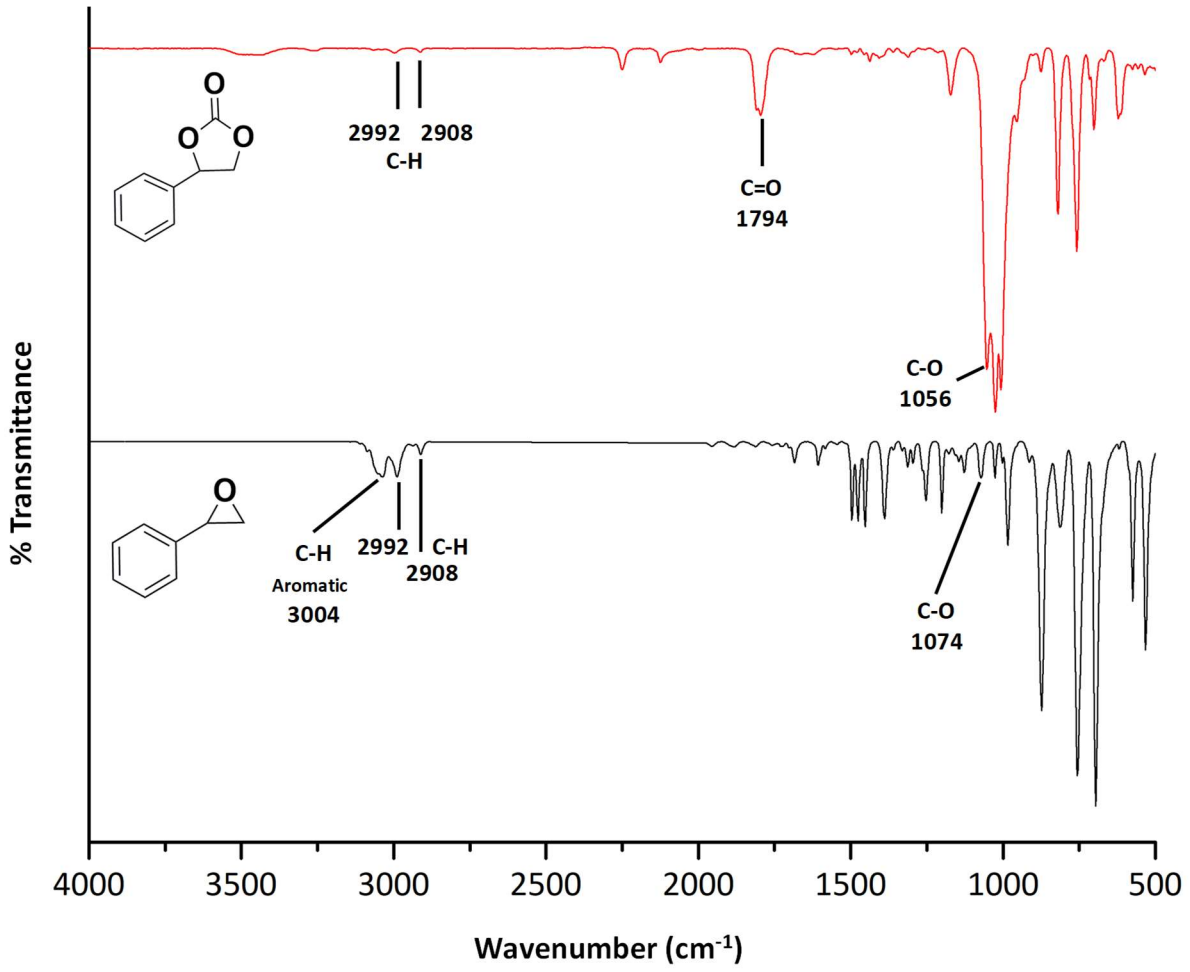

Figure S32. ATR-FTIR spectra of the styrene oxide (black trace) and styrene carbonate (red trace), (Entry 4, Table 3).

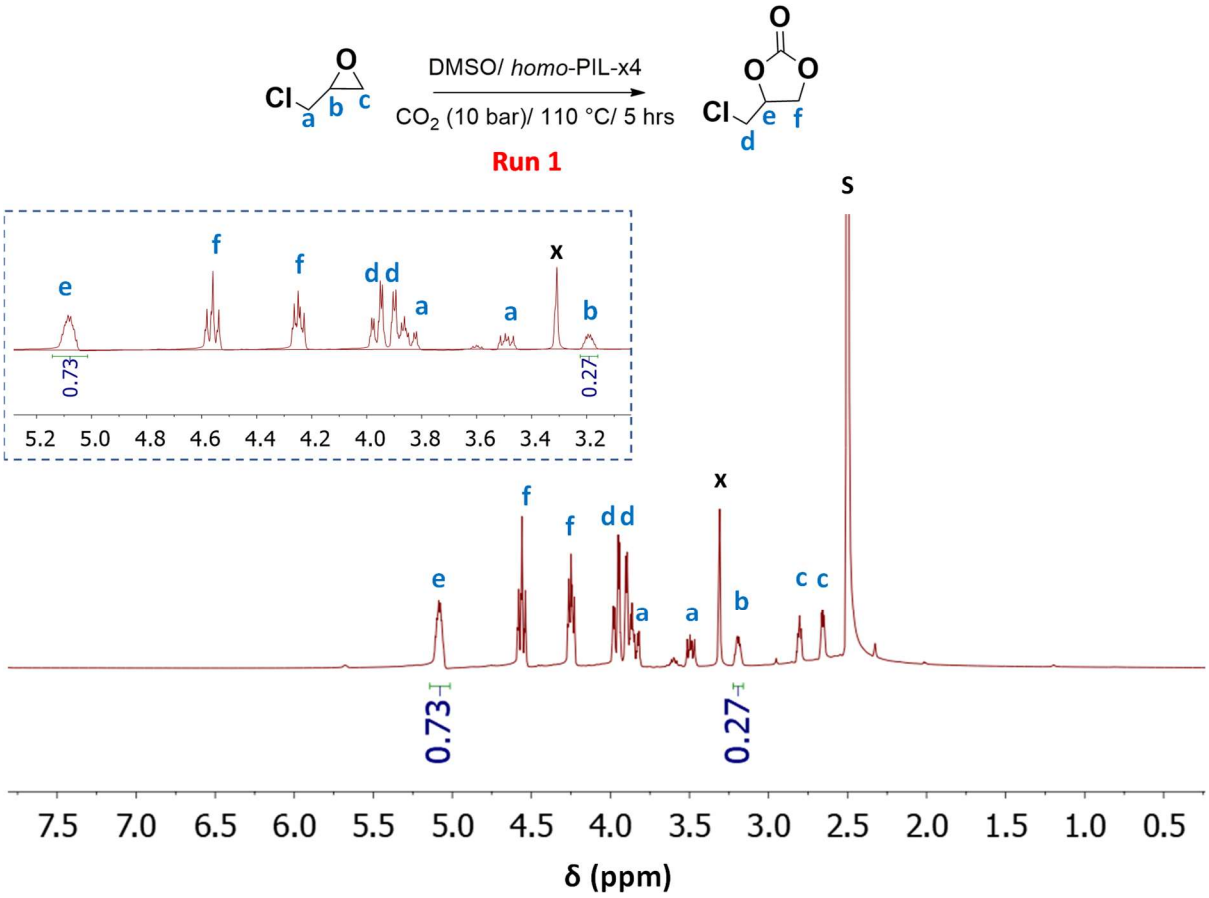

Figure S33. The ^{1}H NMR spectrum of epichlorohydrin carbonate product in DMSO-d_6; **S**: Solvent; **x**: H_2O, catalyzed by *homo*-PIL-x4 at 5 h with a conversion of 73%, first run.

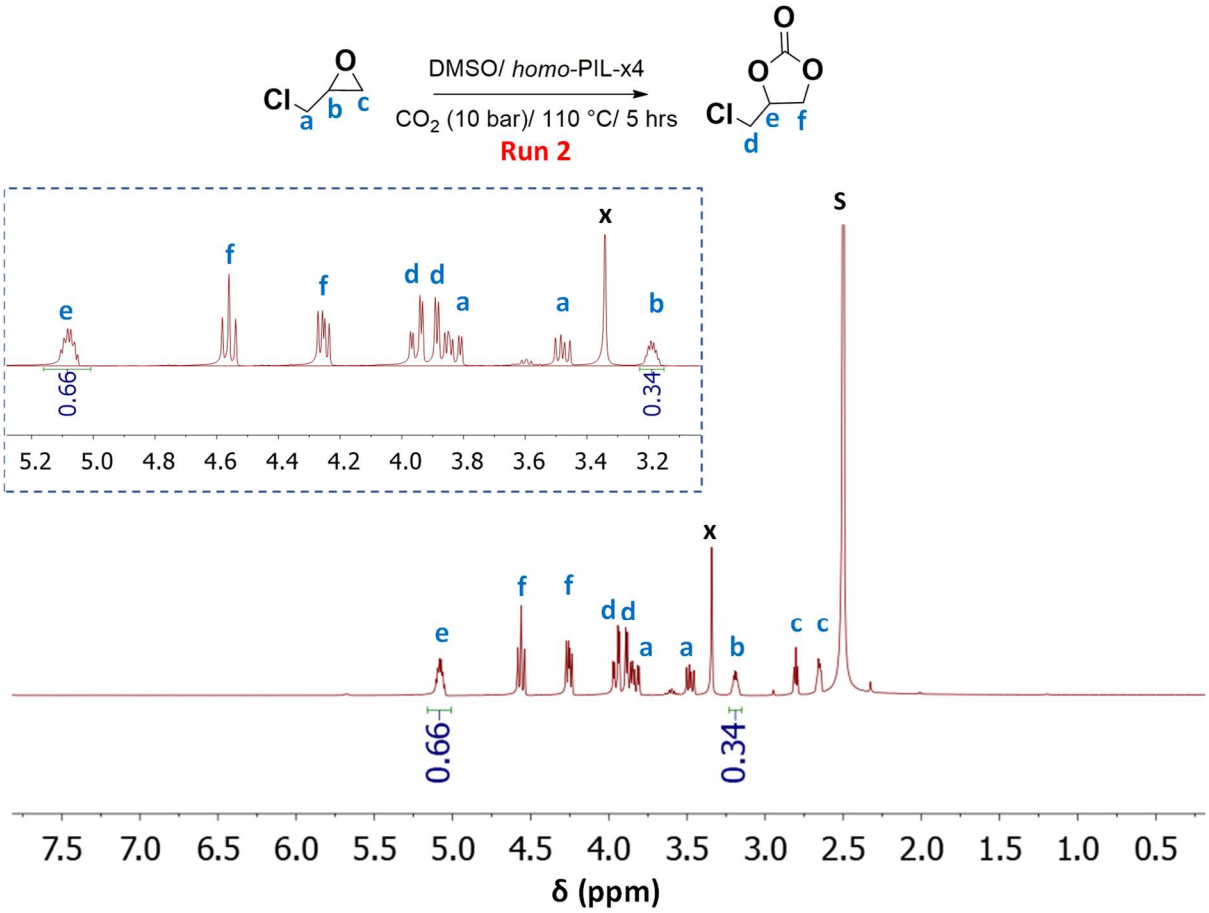

Figure S34. The ^{1}H NMR spectrum of epichlorohydrin carbonate product in DMSO-d_6; **S**: Solvent; **x**: H_2O, catalyzed by *homo*-PIL-x4 at 5 h with a conversion of 66%, second run.

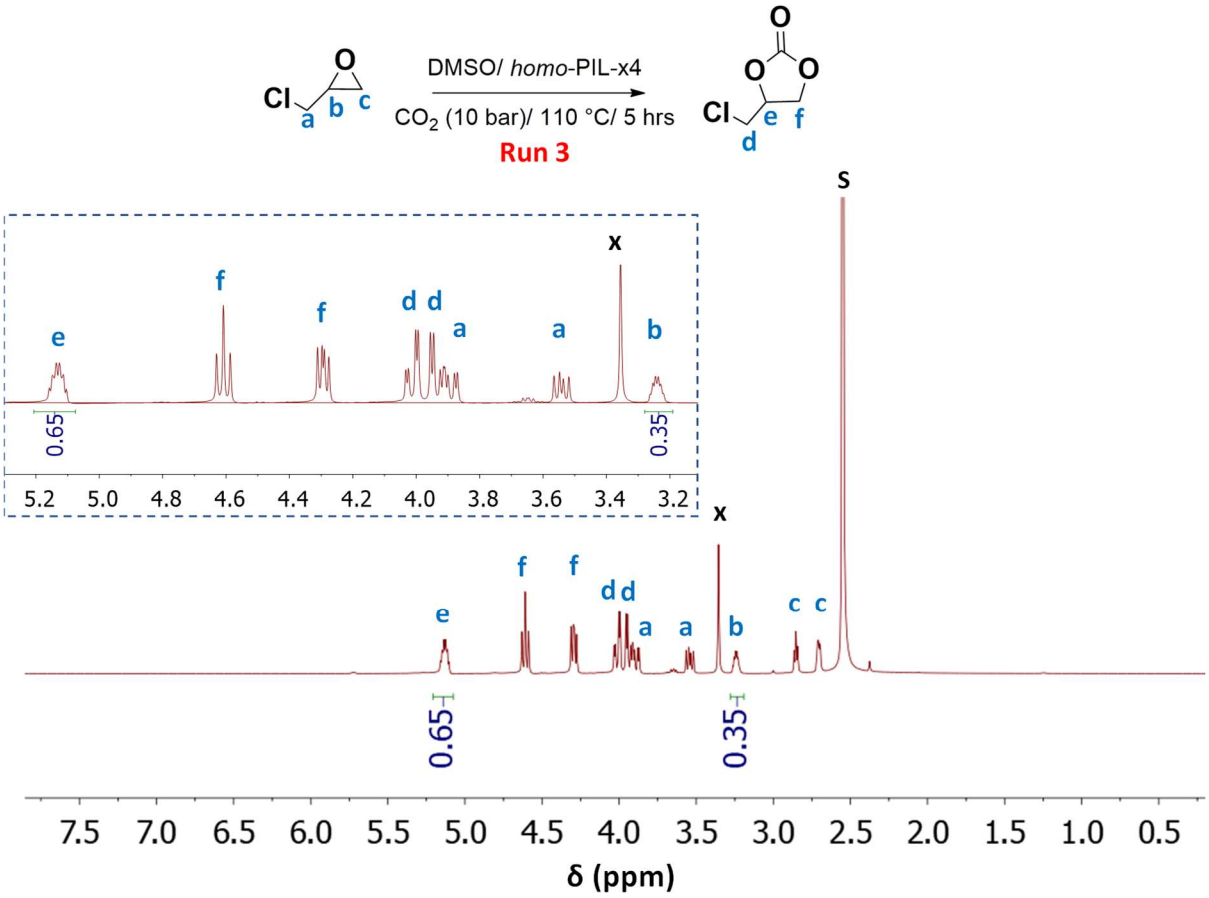

Figure S35. The ^{1}H NMR spectrum of epichlorohydrin carbonate product in DMSO-d_6; **S**: Solvent; **x**: H_2O, catalyzed by *homo*-PIL-x4 at 5 h with a conversion of 65%, third run.

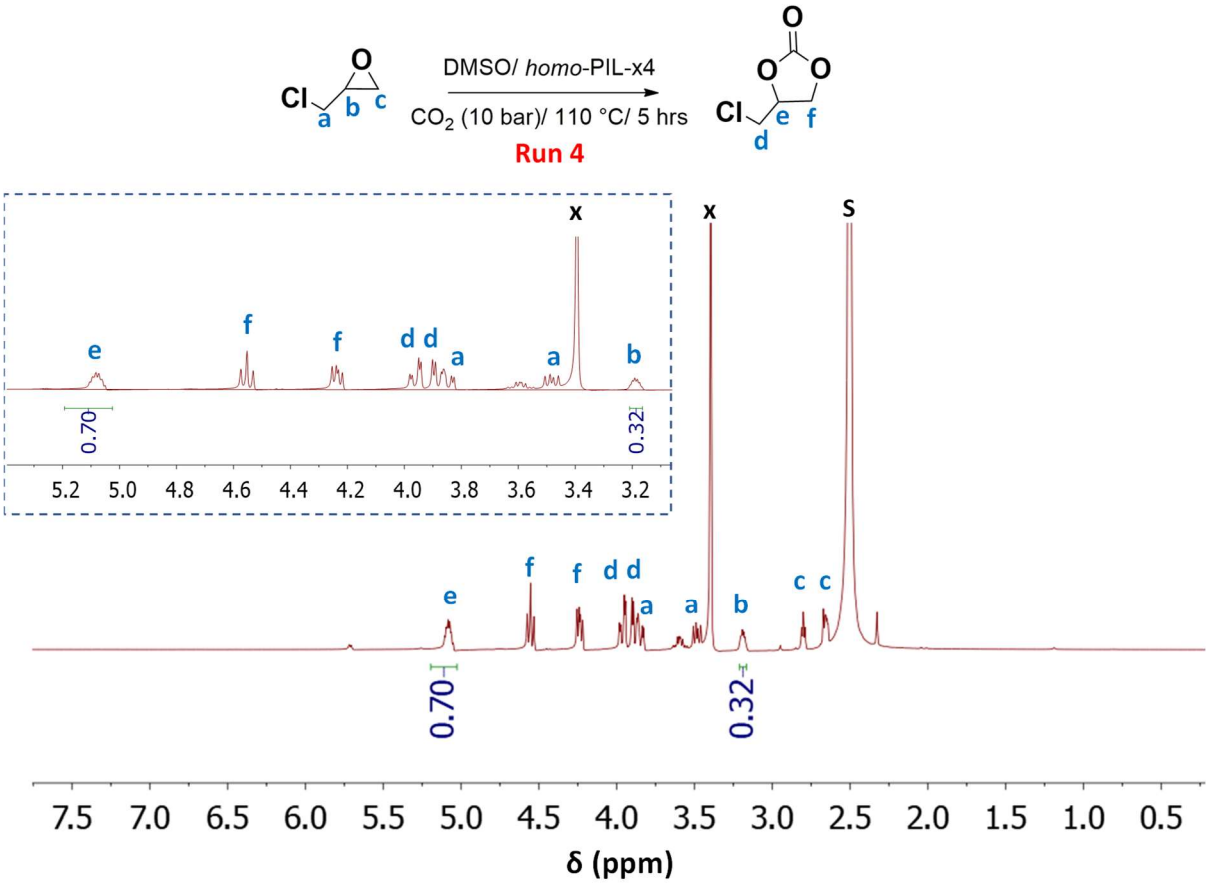

Figure S36. The ^{1}H NMR spectrum of epichlorohydrin carbonate product in DMSO-d_6; **S**: Solvent; **x**: H_2O, catalyzed by *homo*-PIL-x4 at 5 h with a conversion of 70%, fourth run.

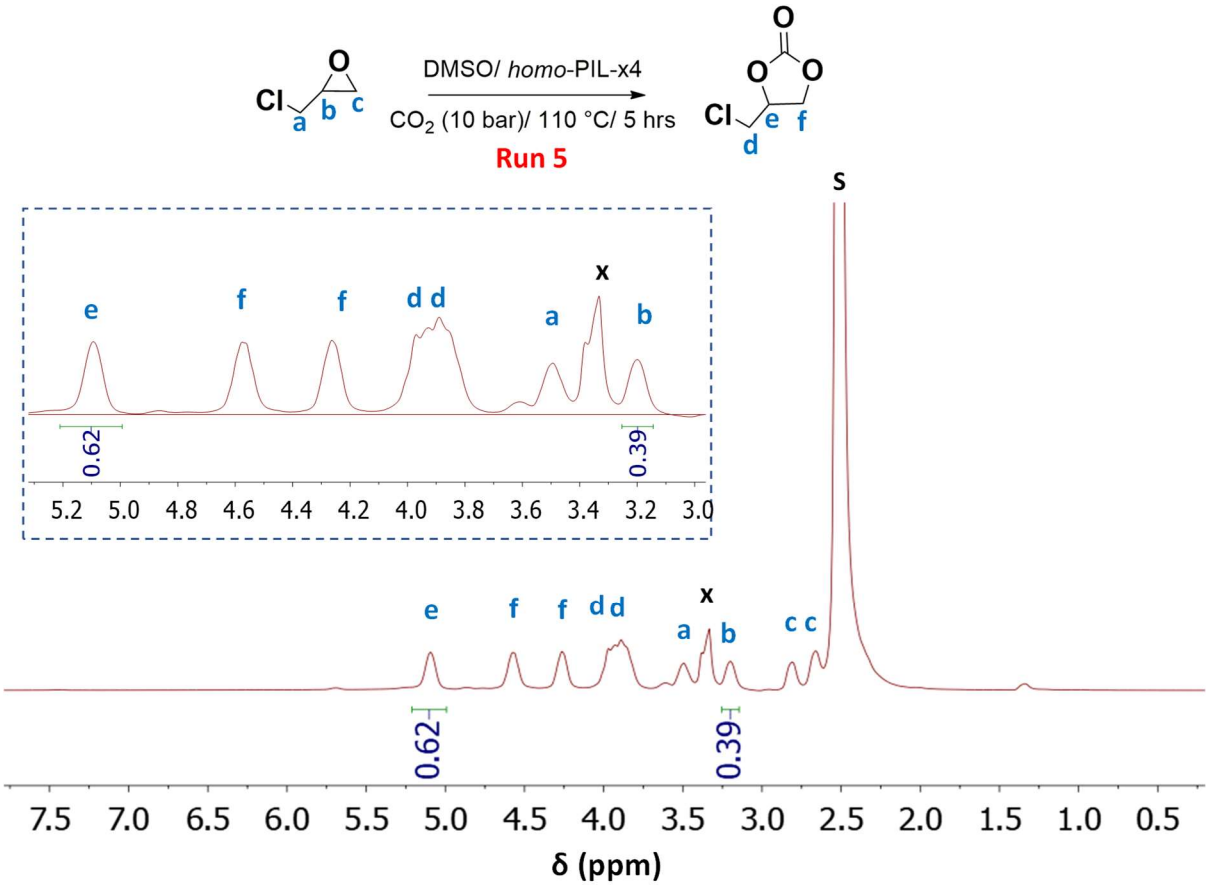

Figure S37. The ^{1}H NMR spectrum of epichlorohydrin carbonate product in DMSO-d_6; **S**: Solvent; **x**: H_2O, catalyzed by *homo*-PIL-x4 at 5 h with a conversion of 62%, fifth run.

References

1 A. Wilke, J. Yuan, M. Antonietti and J. Weber, *ACS Macro Lett.*, 2012, **1**, 1028–1031.
2 X. Feng, C. Gao, Z. Guo, Y. Zhou and J. Wang, *RSC Adv.*, 2014, **4**, 23389–23395.
3 H. Ran, J. Wang, A. A. Abdeltawab, X. Chen, G. Yu and Y. Yu, *J. Energy Chem.*, 2017, **26**, 909–918.
4 M. A. Ziaee, Y. Tang, H. Zhong, D. Tian and R. Wang, *ACS Sustain. Chem. Eng.*, 2018, **7**, 2380–2387.
5 C. Cui, R. Sa, Z. Hong, H. Zhong and R. Wang, *ChemSusChem*, 2020, **13**, 180–187.
6 Y. Xie, J. Liang, Y. Fu, M. Huang, X. Xu, H. Wang, S. Tu and J. Li, *J. Mater. Chem. A*, 2018, **6**, 6660–6666.
7 J. Li, D. Jia, Z. Guo, Y. Liu, Y. Lyu, Y. Zhou and J. Wang, *Green Chem.*, 2017, **19**, 2675–2686.
8 N. Yu. Kuznetsov, R. M. Tikhov, I. A. Godovikov, V. N. Khrustalev and Yu. N. Bubnov, *Org. Biomol. Chem.*, 2016, **14**, 4283–4298.
9 E. I. Privalova, E. Karjalainen, M. Nurmi, P. Mäki-Arvela, K. Eränen, H. Tenhu, D. Yu. Murzin and J.-P. Mikkola, *ChemSusChem*, 2013, **6**, 1500–1509.
10 Q. Zhao, J. C. Wajert and J. L. Anderson, *Anal. Chem.*, 2010, **82**, 707–713.
11 P. Nellepalli, L. C. Tomé, K. Vijayakrishna and I. M. Marrucho, *Ind. Eng. Chem. Res.*, 2019, **58**, 2017–2026.

12 M. A. Ziaee, Y. Tang, H. Zhong, D. Tian and R. Wang, *ACS Sustain. Chem. Eng.*, 2019, **7**, 2380–2387.
13 P. Li, D. R. Paul and T.-S. Chung, *Green Chem.*, 2012, **14**, 1052–1063.
14 R. M. Silverstein, F. X. Webster, D. J. Kiemle and D. L. Bryce, Spectrometric identification of organic compounds, John Wiley and Sons: Hoboken, NJ, 2015
15 J. Hu, Y. Liu, Y. Jiao, S. Ji, R. Sun, P. Yuan, K. Zeng, X. Pu and G. Yang, *RSC Adv.*, 2015, **5**, 16199–16206.
16 N. Li, H. Wang, Q. Xiaosai and Y. Chen, *Mar. Drugs*, 2017, **15**, 223.
17 P. Marzbani, H. Resalati, A. Ghasemian and A. Shakeri, *Bioresources*, 2016, **11**, 8720–8738.
18 A. Abulikemu, G. Halász, A. Csámpai, Á. Gömöry and J. Rábai, *J. Fluor. Chem.*, 2004, **125**, 1143–1146.
19 R. D. McLachlan and R. A. Nyquist, *Spectrochim. Acta Part Mol. Spectrosc.*, 1968, **24**, 103–114.
20 Y. Xie, Z. Zhang, T. Jiang, J. He, B. Han, T. Wu and K. Ding, *Angew. Chem. Int. Ed.*, 2007, **46**, 7255.
21 S. Ghazali-Esfahani, H. Song, E. Păunescu, F. D. Bobbink, H. Liu, Z. Fei, G. Laurenczy, M. Bagherzadeh, N. Yan and P. J. Dyson, *Green Chem.*, 2013, **15**, 1584–1589.
22 T.-Y. Shi, J.-Q. Wang, J. Sun, M.-H. Wang, W.-G. Cheng and S.-J. Zhang, *RSC Adv.*, 2013, **3**, 3726–3732.
23 J. Li, D. Jia, Z. Guo, Y. Liu, Y. Lyu, Y. Zhou and J. Wang, *Green Chem.*, 2017, **19**, 2675–2686.
24 H. Zhong, J. Gao, R. Sa, S. Yang, Z. Wu and R. Wang, *ChemSusChem*, 2020, cssc.202001658.
25 C. Cui, R. Sa, Z. Hong, H. Zhong and R. Wang, *ChemSusChem*, 2020, **13**, 180–187.
26 C. Yang, Y. Chen, Y. Qu, J. Zhang and J. Sun, *Sustain. Energy Fuels*, 2021, **5**, 1026–1033.
27 D. Valverde, R. Porcar, P. Lozano, E. García-Verdugo and S. V. Luis, *ACS Sustain. Chem. Eng.*, 2021, **9**, 2309–2318.